File Cy

AD

TECHNICAL REPORT ARBRL-TR-02293

"MC DRAG" - A COMPUTER PROGRAM FOR ESTIMATING THE DRAG COEFFICIENTS OF PROJECTILES

Robert L. McCoy

February 1981

US ARMY ARMAMENT RESEARCH AND DEVELOPMENT COMMAND
BALLISTIC RESEARCH LABORATORY
ABERDEEN PROVING GROUND, MARYLAND

UNCLASSIFIED

SECURITY CLASSIFICATION OF THIS PAGE (When Data Entered)

REPORT DOCUMENTATION PAGE

READ INSTRUCTIONS BEFORE COMPLETING FORM

1. REPORT NUMBER: TECHNICAL REPORT ARBRL-TR-02293	2. GOVT ACCESSION NO. / 3. RECIPIENT'S CATALOG NUMBER
4. TITLE (and Subtitle): "MC DRAG" - A Computer Program for Estimating the Drag Coefficients of Projectiles	5. TYPE OF REPORT & PERIOD COVERED: Final
	6. PERFORMING ORG. REPORT NUMBER
7. AUTHOR(s): Robert L. McCoy	8. CONTRACT OR GRANT NUMBER(s)
9. PERFORMING ORGANIZATION NAME AND ADDRESS: U.S. Army Armament Research & Development Command U.S. Army Ballistic Research Laboratory (ATTN: DRDAR-BLL) Aberdeen Proving Ground, MD 21005	10. PROGRAM ELEMENT, PROJECT, TASK AREA & WORK UNIT NUMBERS: 1L162618AH80
11. CONTROLLING OFFICE NAME AND ADDRESS: US Army Armament Research and Development Command US Army Ballistic Research Laboratory (DRDAR-BL) Aberdeen Proving Ground, MD 21005	12. REPORT DATE: FEBRUARY 1981
	13. NUMBER OF PAGES: 73
14. MONITORING AGENCY NAME & ADDRESS(if different from Controlling Office)	15. SECURITY CLASS. (of this report): UNCLASSIFIED
	15a. DECLASSIFICATION/DOWNGRADING SCHEDULE

16. DISTRIBUTION STATEMENT (of this Report)

Approved for public release; distribution unlimited.

17. DISTRIBUTION STATEMENT (of the abstract entered in Block 20, if different from Report)

18. SUPPLEMENTARY NOTES

19. KEY WORDS (Continue on reverse side if necessary and identify by block number)

Drag Coefficient	Similarity Rules	"MC DRAG"
Wave Drag	Data Correlation	FORTRAN
Skin Friction Drag	Computer Program	
Base Drag	Drag Estimation	

20. ABSTRACT (Continue on reverse side if necessary and identify by block number)

This report presents a FORTRAN program "MC DRAG" for estimating a projectile's zero-yaw drag coefficient from the given values of certain size and shape parameters. The results are valid over a Mach number range of 0.5 to 5 and a projectile diameter range of 4 to 400 millimetres. A user's guide and a FORTRAN listing of MC DRAG is provided. The program is applied to three illustrative examples: (1) an experimental low-drag small arms bullet, the 5.56mm BRL-1 design; (2) a 55mm scale model of the Minuteman re-entry stage vehicle; (3) the

(continued)

DD FORM 1473, 1 JAN 73 EDITION OF 1 NOV 65 IS OBSOLETE

UNCLASSIFIED

SECURITY CLASSIFICATION OF THIS PAGE (When Data Entered)

155mm long-range artillery shell M549. The MC DRAG program estimates drag coefficient to within 3% error (1σ) at supersonic speeds, 11% error at transonic speeds, and 6% error at subsonic speeds.

TABLE OF CONTENTS

LIST OF ILLUSTRATIONS

LIST OF ILLUSTRATIONS

LIST OF SKETCHES

I. INTRODUCTION

Since World War II, there has been an ever increasing need for faster and more accurate methods of estimating the aerodynamic properties of aircraft, missiles and ordnance projectiles. Prior to the last decade, this need was met by systematic compilations of available data, by calculations based on theoretical flowfield solutions, and by combinations of the above.

In recent years the proliferation of large and powerful computing machinery has generated widespread interest in implementing faster, more uniform, and more accurate aerodynamic estimates. Approaches based on flowfield calculation[1,2] offer the long range prospect of improved accuracy and uniformity of approximation for arbitrary projectile shapes. However, even with the more advanced computers, this approach is usually quite lengthy, applicable only over specified ranges of Mach number, Reynolds number and yaw level, and difficult to apply to real, non-smoothly contoured ordnance projectile shapes.

Aerodynamic data can always be fitted to polynomials; the process is rapid--even on modest-size computers--and often produces extremely good fits[3,4]. However, it is inherently dangerous to extrapolate such polynomial fits beyond the original data base. When extrapolation is required, the data should be fitted to equations founded on theory and valid across the extrapolated region.

In this report, a relationship between the zero yaw drag coefficient and Mach number is obtained from certain aerodynamic similarity rules. This relationship involves (a) certain shape and size parameters and (b) additional parameters whose values have been determined by least squares.

---

1. *F. G. Moore, "Body Alone Aerodynamics of Guided and Unguided Projectiles at Subsonic, Transonic and Supersonic Mach Numbers," Naval Weapons Laboratory Technical Report TR-2796, November 1972. (AD 754098)*

2. *R. L. McCoy, "Estimation of the Static Aerodynamic Characteristics of Ordnance Projectiles at Supersonic Speeds," Ballistic Research Laboratories Report 1682, November 1973. (AD 771148)*

3. *R. H. Whyte, "SPIN-73, An Updated Version of the Spinner Computer Program," Picatinny Arsenal Contractor Report TR-4588, November 1973. (AD 915628L)*

4. *E. S. Sears, "An Empirical Method for Predicting Aerodynamic Coefficients for Projectiles - Drag Coefficient," Air Force Armament Laboratory Technical Report TR-72-173, August 1972. (AD 904587L)*

These least square values are valid over a Mach number range of 0.5 to 5 and a projectile diameter range of 4 to 400mm. Thus, within these ranges, the drag coefficient can be computed directly - that is, without any additional fitting process - for a given set of size and shape parameters. The program MC DRAG performs this computation. The program will be applied to three illustrative examples: a small arms bullet, a re-entry vehicle model, and an artillery shell.

II. THE PHYSICAL NATURE OF DRAG

The simplest approach to separation of drag into component parts is to examine forces normal to the projectile surface and those tangential to the surface. The drag arising from pressure forces acting normal to the surface we call pressure drag, or wave drag, and the tangential drag force due to viscosity we call viscous drag, or skin friction drag. For a projectile consisting of a nose, a cylindrical afterbody, a rotating band, and a boattail or conical flare tail, the pressure drag is the sum of the pressure drag forces due to each projectile component. Thus, our zero-yaw drag coefficient takes the form:

$$C_{D_O} = C_{D_H} + C_{D_{BT}} + C_{D_B} + C_{D_{RB}} + C_{D_{SF}} ,$$

where C_{D_O} = total drag coefficient at zero angle of attack

C_{D_H} = pressure drag coefficient due to projectile head (nose)

$C_{D_{BT}}$ = pressure drag coefficient due to boattail (or flare)

C_{D_B} = pressure drag coefficient due to the blunt base

$C_{D_{RB}}$ = pressure drag coefficient due to a rotating band

$C_{D_{SF}}$ = skin friction drag coefficient due to the entire projectile wetted surface (excluding the base)

The behavior of all the above components of drag is strongly dependent on free stream Mach number; the skin friction drag and the base drag depend on Reynolds number as well. Some general comments can be made about the behavior of specific drag components in various speed regimes.

The pressure drag is associated with the amount of energy necessary to continuously form the wave system as the projectile moves through the air. At sufficiently low (incompressible) speeds, the net pressure drag acting over the projectile wetted surface, including the base, obeys d'Alembert's paradox; if the fluid is inviscid, the drag is zero. However, the near wake of a blunt-based body is a region of separated flow; hence, a base drag is experienced by the projectile even at incompressible speeds.

As the projectile speed is increased, the effects of compressibility begin to appear. Since more energy must be supplied to maintain a wave system in a compressible fluid, the drag begins to rise. Eventually a free stream speed will be reached that produces local sonic flow at some point on the projectile, and this speed marks the beginning of the transonic regime. Further increases in speed are accompanied by the formation of shock waves, which require significantly more energy to maintain, and the effect on drag is a sharp rise after the first appearance of shocks. Finally, a free stream speed is reached above which the local flow speed along the surface is everywhere supersonic, and this speed marks the beginning of the supersonic regime.

In summary, the pressure drag coefficient, exclusive of the base, is zero at low subsonic speeds, rises sharply at transonic speeds, then slowly decreases with increasing supersonic speeds. The near wake behind a blunt-based projectile is a reduced pressure region, or partial vacuum. At very low subsonic speeds, the base pressure is only slightly less than free stream static pressure; at sufficiently high supersonic speeds, the base pressure approaches zero. Thus, the base drag coefficient is important in all flow regimes.

The skin friction drag of a projectile depends primarily on Reynolds number, and to a lesser extent on compressibility. A projectile with a fully turbulent boundary layer will experience a significantly higher skin friction drag than one with a laminar boundary layer. In either case, increasing free stream speed decreases the skin friction drag coefficient.

The qualitative behavior of the various components of the drag coefficient for a typical artillery projectile is shown in Sketch 1.

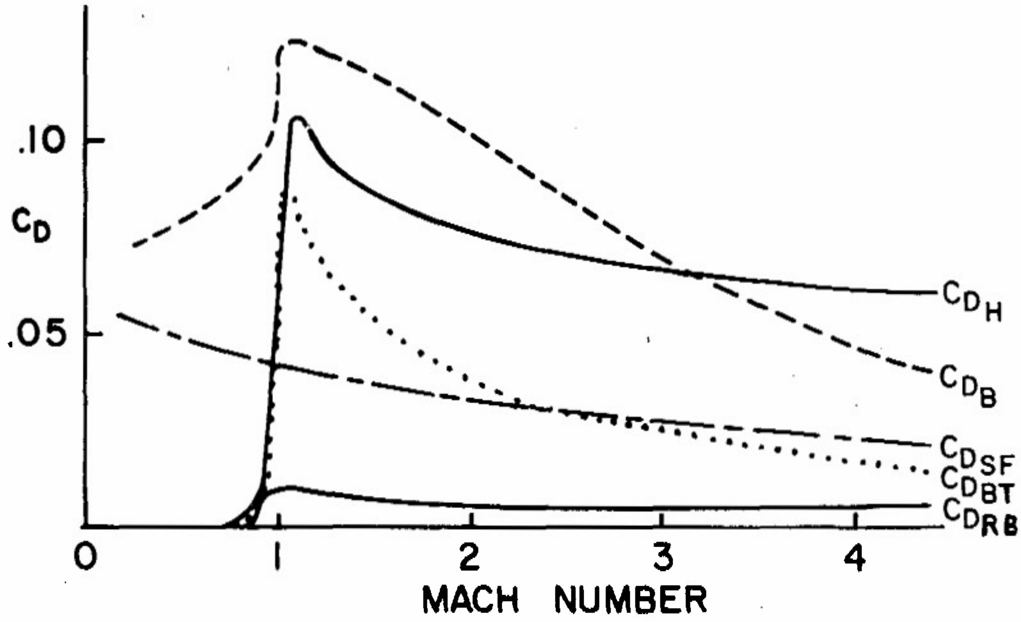

Sketch 1. Behavior of the Various Components of Drag

In the following sections, similarity parameters suitable for correlating the various individual components of drag are examined in detail.

III. PRESSURE DRAG COEFFICIENT FOR A PROJECTILE NOSE

The wave drag of a pointed conical nose at supersonic speeds is well known from Taylor-Maccoll theory[5], and the head drag coefficients of conical noses can be readily correlated with Mach number by means of Göthert's similarity rule[6]:

$$C_{D_H}\ (M_\infty^{\ 2}-1) = f\ (\tau\sqrt{M_\infty^{\ 2}-1},\ \tau), \qquad (1)$$

where $\tau = \frac{1}{L_N}$, or thickness ratio

M_∞ = free stream Mach number

5. *G. I. Taylor and J. W. Maccoll, "The Air Pressure on a Cone Moving at High Speeds," Proc. Roy. Soc. A., Vol. 139 (1933), pp. 278-311.*

6. *M. J. Van Dyke, "The Similarity Rules for Second-Order Subsonic and Supersonic Flow," NACA Technical Note 3875, October 1956.*

L_N = length of conical head (calibers)

f( ) means a function of ( )

Equation (1) also correlates the head drag coefficient with Mach number for pointed ogival noses. Conical flow results for a wide range of free stream Mach numbers and thickness ratios are available[7], and a number of unpublished calculations for pointed ogives have been performed at BRL using the method of characteristics and second-order perturbation theory[2]. Over the Mach number range from one to four, and for thickness ratios less than two, the following correlation was obtained using non-linear squares:

$$C_{D_H} (M_\infty^2-1) = (C_1-C_2\tau^2) \left[\tau\sqrt{M_\infty^2-1}\right]^{(C_3+C_4\tau)} \qquad (2)$$

where $C_1 = .7156 - .5313(R_T/R) + .5950(R_T/R)^2$

$C_2 = .0796 + .0779(R_T/R)$

$C_3 = 1.587 + .049(R_T/R)$

$C_4 = .1122 + .1658(R_T/R)$

The quantity (R_T/R) is a headshape parameter; it is the ratio of the tangent radius for the same head length to the actual ogive radius. Thus $(R_T/R) = 0$ for a cone, $(R_T/R) = 1$ for a tangent ogive nose, and values between 0 and 1 describe various secant-ogive shapes.

The standard deviation of the fit of Equation (2) is 5% in C_{D_H}; since C_{D_H} represents approximately 40% of the total C_{D_0} for typical projectiles, the use of this equation will result in less than 2% error in estimating total drag coefficient at supersonic speeds. Figure 1 shows the correlation of the available data with Equation (2). The flagged symbols in Figure 1 are for noses shorter in length than one caliber, and these blunt noses represent the largest errors in using Equation (2). If thickness ratio is restricted to be less than one, the standard errors quoted above will be reduced by a factor of two.

---

7. *R. F. Clippinger, J. H. Giese and W. C. Carter, "Tables of Supersonic Flows About Cone Cylinders; Part I, Surface Data," Ballistic Research Laboratories Report 729, July 1950.*

Equation (2) can be readily modified to account for the effects of leading edge bluntness. For a blunt leading edge (mêplat), let the originally pointed nose be opened up to a mêplat diameter, d_M, as shown in Sketch 2.

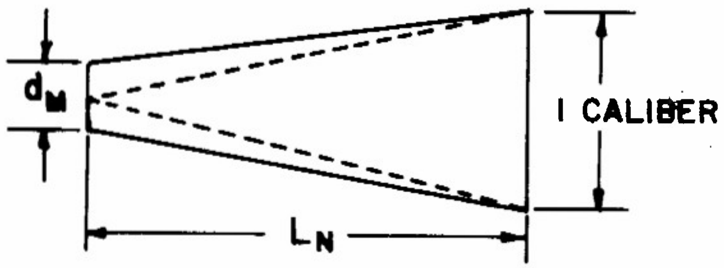

Sketch 2. Geometry of a Blunt Leading Edge Nose

Since thickness ratio, τ, equals twice the average slope along the nose, τ can be redefined as:

$$\tau = \frac{1 - d_M}{L_N} \quad , \tag{3}$$

where d_M is mêplat diameter (calibers). In addition to the redefinition of τ, Equation (2) must be corrected by adding to C_{D_H} the effect of stagnation pressure acting on the flat leading face of the blunted nose. Equation (2) with τ redefined and the stagnation pressure correction added becomes:

$$C_{D_H} = \left(\frac{C_1 - C_2\tau^2}{M_\infty^{\,2} - 1}\right) \left[\tau\sqrt{M_\infty^{\,2} - 1}\,\right]^{(C_3 + C_4\tau)} + \frac{\pi}{4} K \, d_M^{\,2} \, C_{P_s} \quad , \tag{4}$$

where C_{P_s} is the stagnation pressure coefficient, and K is a correction for pressure "leakage" off the flat face. Charters and Stein[8] suggested

8. *A. C. Charters and H. Stein, "The Drag of Projectiles with Truncated Cone Headshapes," Ballistic Research Laboratories Report 624, March 1952. (AD 800468)*

a value of 0.9 for K. Dickinson[9] reported the experimental results of méplat firings with both conical and ogival noses. A least squares fit of the data of reference 9 to Equation (4) yields a value of 0.75 for K at supersonic speeds. The correlation is shown in Figure 2.

The recent successful attack on axisymmetric transonic flows by Wu, Aoyama, and Moulden[10] at the University of Tennessee Space Institute provides the background for an attempt at transonic data correlations. The similarity rule for the head drag coefficient of slender transonic noses was derived by Cole, Solomon, and Willmarth[11]:

$$\frac{C_{D_H}}{\tau^3} + \ln \tau = f \left[\frac{M_\infty{}^2-1}{(\gamma+1)M_\infty{}^2\tau^2}\right] \qquad (5)$$

Wu, Aoyma, and Moulden measured pressure distributions along slender ogival noses and showed good agreement between their numerical solution of the transonic small disturbance equation and experiment. Equation (5) correlates the head drag and thickness ratio data of reference 10 very well, since the data were taken only for slender noses. At $M_\infty = 1$, Equation (5) predicts a correlation of C_{D_H} with $-\tau^3 \ln\tau$ as shown in Sketch 3.

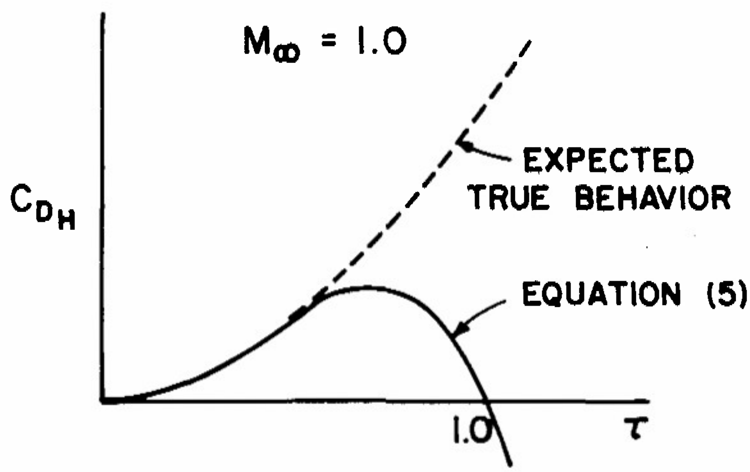

Sketch 3. Slender-Body Correlation of Transonic Wave Drag

---

9. *E. R. Dickinson, "Some Aerodynamic Effects of Blunting a Projectile Nose," Ballistic Research Laboratories Memorandum Report 1596, September 1964. (AD 451977)*

10. *J. M. Wu, K. Aoyama, and T. H. Moulden, "Transonic Flow Fields Around Various Bodies of Revolution Including Preliminary Studies on Viscous Effects With and Without Plume," U. S. Army Missile Command Report RD-TR-71-12, May 1971. (AD 729335)*

11. *J. D. Cole, G. E. Solomon, and W. W. Willmarth, "Transonic Flows Past Simple Bodies," Journal of the Aeronautical Sciences, Vol. 20, No. 9, 1953, pp. 627-634.*

The slender-body similarity rule is obviously invalid for thickness ratios of order 1, and, since many real vehicles are this blunt, a better rule is needed.

Von Kármán[12] derived a two-dimensional transonic similarity rule using the exact equation from perturbation theory, hence not inherently restricted to slender profiles. Von Kármán's rule, in a slightly different form, is:

$$\frac{C_{D_H}\left[(\gamma+1)M_\infty^2\right]^{1/3}}{\tau^{5/3}} = f\left(\frac{M_\infty^2-1}{\left[(\gamma+1)M_\infty^2\tau\right]^{2/3}}\right) \tag{6}$$

Analogy between the two- and three-dimensional rules for supersonic flows suggested the following form for an axisymmetric transonic similarity rule:

$$C_{D_H} = F(\tau^n) + f\left[\frac{\tau(M_\infty^2-1)}{(\gamma+1)M_\infty^2}\right] \tag{7}$$

From the data of reference 10 at $M_\infty = 1$, the head drag coefficient is found to vary as $\tau^{9/5}$. A least squares fit of the transonic head drag coefficient yields the result:

$$C_{D_H} = .368\tau^{9/5} + \frac{1.6\tau(M_\infty^2-1)}{(\gamma+1)M_\infty^2}\ , \tag{8}$$

valid for $M_\infty > M_c$, where $M_c = [1 + .552\tau^{4/5}]^{-1/2}$.

The correlation of the transonic head drag data of reference 10 with thickness ratio and Mach number is shown in Figure 3.

IV. PRESSURE DRAG COEFFICIENT FOR A BOATTAIL

The form of a similarity law for supersonic boattail drag was suggested by expanding the second-order small disturbance equation in series, for small values of the boattail angle, β. The result is:

$$[C_{D_{BT}}] = \frac{4A\tan\beta}{k}\{(1-e^{-kL_{BT}}) + 2\tan\beta\,[e^{-kL_{BT}}(L_{BT} + \frac{1}{k}) - \frac{1}{k}]\} \tag{9}$$

---

12. *H. W. Liepmann and A. Roshko, Elements of Gasdynamics, John Wiley and Sons, 1957.*

where $[C_{D_{BT}}]$ is the similarity parameter

β = Boattail angle (β is negative for a conical flare tail)

L_{BT} = Boattail length (calibers)

A = Change in boattail pressure coefficient due to a Prandtl-Meyer expansion

k = Boattail pressure recovery factory

The form of the terms A and k in Equation (9) also resulted from second-order theory, but contained unknown coefficients, which were obtained from least squares fitting of boattail drag coefficients calculated by the method of characteristics. The results for the terms A and k are:

$$A = A_1 e^{-\sqrt{\frac{2}{\gamma M_\infty^2}} L_{CYL}} + \frac{2\tan\beta}{\sqrt{M_\infty^2-1}} - \frac{[(\gamma+1)M_\infty^4 - 4(M_\infty^2-1)]\tan^2\beta}{2(M_\infty^2-1)^2}$$

$$A_1 = [1 - \frac{3(R_T/R)}{5M_\infty}] \{\frac{5\tau}{6\sqrt{M_\infty^2-1}} (\frac{\tau}{2})^2 - \frac{.7435}{M_\infty^2} (\tau M_\infty)^{1.6}\}$$

$$k = \frac{.85}{\sqrt{M_\infty^2-1}}$$

L_{CYL} = Length of projectile cylinder section (calibers)

A_1 = Headshape correction factor for supersonic boattail drag coefficient

Experimental boattail drag coefficient values were obtained by numerical integration of measured pressure distributions along conical boattails[13],[14]. Figure 4 shows the correlation of boattail drag coefficient with $[C_{D_{BT}}]$ for supersonic speeds.

No similarity parameter applicable to boattails at transonic speeds could be found in the literature, and, lacking anything else, a

13. *R. Sedney, "Review of Base Drag," Ballistic Research Laboratories Report 1337, October 1966. (AD 808767)*

14. *J. Huerta, "An Experimental Investigation at Supersonic Mach Numbers of Base Drag of Various Boattail Shapes with Simulated Base Rocket Exhaust," Ballistic Research Laboratories Memorandum Report 1983, June 1969. (AD 855156)*

modification of the form used for supersonic boattails was tried. Sykes[15] has measured pressure distribution on transonic boattails, and integrated the pressures to obtain boattail drag coefficient values. A fairly good correlation of Sykes' data was found with the similarity parameter:

$$[C_{D_{BT}}] = 4\tan^2\beta\,(1+\tfrac{1}{2}\tan\beta)\,\{1-e^{-2L_{BT}} + 2\tan\beta\,[e^{-2L_{BT}}\,(L_{BT}+\tfrac{1}{2}) - \tfrac{1}{2}]\} \qquad (10)$$

The correlation must be performed for fixed Mach numbers, since no explicit Mach number dependence appears in Equation (10). Figure 5 shows the correlation of Sykes' data for three transonic Mach numbers; the correlation line for $M_\infty = 0.9$ is omitted from the figure since it nearly coincides with the line for $M_\infty = 1.1$. The transonic boattail drag correlation is obviously not as good as that obtained at supersonic speeds.

V. PRESSURE DRAG COEFFICIENT FOR A ROTATING BAND

Moore[1] conducted wind tunnel tests to determine the effect of a rotating band on drag. Figure 6 shows the variation of rotating band drag coefficient with Mach number. The drag coefficient increment for a band is found by multiplying the curve of Figure 6 by $(d_{RB} - 1)$, where d_{RB} is the rotating band diameter, in calibers.

The rotating band is assumed to be located near the aft end of the projectile cylindrical section, and a small error will result from using the curve of Figure 6 to estimate the drag of a band located farther forward on the projectile. The prediction of rotating band drag could be improved by obtaining more experimental data on the effects of band configuration and location. However, the band contributes less than 5% of total drag on typical projectiles; hence refinement in the band drag estimate is probably unjustified.

VI. SKIN FRICTION DRAG COEFFICIENT

The skin friction drag coefficient, $C_{D_{SF}}$, is given by;

$$C_{D_{SF}} = \frac{4}{\pi} C_F S_W , \qquad (11)$$

where C_F = skin friction coefficient for a smooth flat plate

---

15. *D. M. Sykes, "Experimental Investigation of the Pressures on Boat-Tailed Afterbodies in Transonic Flow with a Low-Thrust Jet," Royal Armament Research and Development Establishment Memorandum 39/70, Fort Halstead, Kent, England, December 1970.*

S_W = projectile wetted surface area, exclusive of the base (calibers^2)

For a laminar boundary layer, the Blasius formula[16], with a correction for the effect of compressibility is:

$$C_{f_L} = \frac{1.328}{\sqrt{Re_\ell}} (1 + .12M_\infty^2)^{-.12} , \qquad (12)$$

where C_{f_L} = laminar skin friction coefficient

Re_ℓ = Reynolds number, based on projectile length

Prandtl's empirical formula[16] for a fully turbulent boundary layer, corrected for compressibility, is:

$$C_{f_T} = \frac{.455}{(\log_{10} Re_\ell)^{2.58}} (1 + .21M_\infty^2)^{-.32} , \qquad (13)$$

where C_{f_T} = turbulent skin friction coefficient

Schlichting[16] shows good agreement between Equation (13) and Van Driest's more complete theory[17] for compressible turbulent boundary layers adjacent to an adiabatic wall. Equation (13) is much easier to use than Van Driest's result, which requires an iterative numerical solution; hence (13) is selected for the present theory.

The wetted surface area of the projectile nose is given by the approximation:

$$S_{W_{nose}} = \frac{\pi}{2} L_N \left(1 + \frac{1}{8L_N^2}\right) \left[1 + \left(\frac{1}{3} + \frac{1}{50L_N^2}\right) (R_T/R)\right] \qquad (14)$$

For the mild boattails or conical flares permitted in the present theory, the difference in wetted surface area between the actual boattail or flare and that of an equivalent length circular cylinder is negligible. Hence the wetted surface area of the projectile afterbody is approximated by:

---

16. *H. Schlichting, Boundary Layer Theory, McGraw-Hill, 1955.*

17. *E. R. Van Driest, "Turbulent Boundary Layers in Compressible Fluids," Journal of the Aeronautical Sciences, Vol. 18, No. 3, 1951, pp. 145-160, 216.*

$$S_{w_{cyl}} = \pi(L_T - L_N) \quad , \tag{15}$$

where L_T = overall length of projectile (calibers)

The Reynolds number, based on projectile total length, is:

$$Re_\ell = \frac{U_\infty \ell}{\nu} \quad , \tag{16}$$

where U_∞ = velocity of the free stream

ℓ = total length of projectile

ν = kinematic viscosity

Since $U_\infty = a_\infty M_\infty$, where a_∞ is speed of sound in air, and $\ell = L_T d_{REF}$, where d_{REF} is reference diameter of the projectile, the Reynolds number can be written:

$$Re_\ell = 23296.3\ M_\infty L_T\ d_{REF} \quad , \tag{17}$$

where d_{REF} must be in millimetres (mm)

Equation (17) gives the Reynolds number for sea-level conditions at a temperature of 15°C.

The skin friction drag coefficient is computed for a fully laminar boundary layer, and for a fully turbulent boundary layer, and a weighted average taken, depending on the approximate location of transition. For most ordnance projectiles, transition occurs either near the end of the nose, or near the leading edge. Hence only two options are provided for the character of the boundary layer: (1) a fully turbulent case, and (2) laminar flow on the nose and turbulent flow on the afterbody. This is a user-specified option. Experience suggests that option (2) should be specified for smooth projectiles under 20mm in diameter, and option (1) for larger shell, but no infallible rule exists for making this decision. Inspection of a spark shadowgraph of the projectile in question is the most reliable method.

VII. BASE DRAG COEFFICIENT

Accurate estimation of the base drag coefficient requires an equally accurate estimate of the ratio of base pressure to free stream static pressure. Chapman[18] showed that for square-based projectiles at supersonic speeds, the base pressure depends strongly on local approach Mach number and on the character of the boundary layer just upstream of the base. Most ordnance projectiles have turbulent boundary layers in the vicinity of the base, and in reference 2 the author illustrated a method of correcting the base pressure for boattail effects at supersonic speeds. The method used in reference 2 breaks down at low supersonic speeds; in addition, the present theory is designed to include drag estimates at transonic and subsonic speeds, where the theory of reference 2 is inapplicable.

No similarity parameter for correlating base pressure data could be found in the literature, and for the present purpose a limited study was performed to determine an empirical result that accurately described the existing data.

A large amount of high quality free flight total drag data is available at BRL from the firings of various models through the spark photography ranges. The approach used to determine effective base pressure in the present study consisted of estimating all the other contributions to drag by the methods outlined previously in Sections III and IV, and subtracting from the measured total drag coefficients. An average base pressure was then inferred from the derived base drag coefficient. The ratio of inferred base pressure, P_B, to free stream static pressure, p_∞, was found to correlate well with the empirical similarity parameter:

$$\left[\frac{P_B}{p_\infty}\right] = \left[1 + .09M_\infty^2 \left(1 - e^{-L_{CYL}}\right)\right] \left[1 + \tfrac{1}{4}M_\infty^2 \left(1-d_B\right)\right], \tag{18}$$

P_B = Base pressure

p_∞ = Free stream static pressure

d_B = Projectile base diameter (calibers)

An attempt to correlate the effective base pressure data with Reynolds number did not yield a significant correlation. Although this result contradicts that found in references 2 and 18, the correlation of the data with Equation 18 is sufficiently good to justify neglecting Reynolds number effects.

A plot of $\left[\frac{P_B}{p_\infty}\right]$ versus free stream Mach number is shown in Figure 7. The plotted data points are averages of all available experimental

---

18. *D. R. Chapman, "An Analysis of Base Pressure at Supersonic Velocities and Comparison with Experiment," NACA Report 1051, 1951.*

data at the indicated Mach number. The correlation is valid for boattail lengths up to 1.5 calibers, and for base diameters as small as 0.65 caliber.

The solid curve of Figure 7 was determined from a least squares fit of the data. The estimate of base drag coefficient is now obtained from the relation:

$$C_{D_B} = \frac{2d_B^{\,2}}{\gamma M_\infty^{\,2}} \left(1 - \frac{P_B}{P_\infty}\right) , \qquad (19)$$

where C_{D_B} = Base drag coefficient

The previous discussions on boattail drag and base drag coefficients refer only to conical boattails. It should be noted that the present theory also predicts total drag coefficients accurately for conical flare tails ($d_B > 1$). This result provides a reasonable degree of assurance that the semi-empirically derived similarity parameters for boattail and base drag coefficients have some correspondence with physical reality.

VIII. COMPARISON OF THE PRESENT THEORY WITH EXPERIMENT

In late December 1974, the author combined the results discussed in Sections III through VII of this report into a FORTRAN IV computer program, designed to provide rapid estimates of the drag coefficients of ordnance projectiles. Before the program could be released for general use, it had to be validated by comparison with experiment, for a fairly large sample of previously tested configurations. G. Paul Neitzel, Jr., of the Free Flight Aerodynamics Branch, was given a copy of the program and asked to assist in this task. Neitzel compared the present theory and that of reference 1 with spark range data he had recently obtained[19] for the 30mm Hispano-Suiza HS831-L practice round; he also suggested the name "MC DRAG" for the program, and this name was adopted by other members of the Laboratory.

---

19. *G. P. Neitzel, Jr., "Aerodynamic Characteristics of 30mm HS831-L Ammunition Used in the British 30mm Rarden Gun," Ballistic Research Laboratories Memorandum Report 2466, March 1975. (AD B003797L)*

It would be impractical to include detailed comparisons of the present theory with experiment for all the configurations that have been checked. Therefore, a few cases are presented to demonstrate the ability of the program to properly predict the effects of systematic changes in projectile configuration on drag. In addition, several actual designs of recent or current interest are considered, and, finally, a standard error curve is presented, which represents the performance of the MC DRAG program compared with a large volume of available BRL free-flight drag data on bodies of revolution.

Dickinson[9,20,21,22] conducted a series of experimental programs in the BRL spark photography ranges to determine the influence of systematic configuration changes on the aerodynamic characteristics of projectiles. In reference 20, the effect of headshape variation at $M_\infty = 2.44$ was investigated. Figure 8 shows the comparison of the present theory with the experimental data of reference 20.

In reference 21, Dickinson reported the effects of varying head length and body length at $M_\infty = 1.8$, for both conical and secant-ogival nose shapes. Figure 9 shows the comparison of the present theory with experiment for the effects of added afterbody length, and Figure 10 is a similar comparison for head length effects.

Figure 11 compares the theoretical and experimental[22] effects of varying boattail length on a cone-cylinder projectile at high supersonic speeds. Figure 12 is a similar comparison for boattail effects on a 7-caliber long tangent-ogive nose projectile[23] at $M_\infty = 1.7$.

---

20. *E. R. Dickinson, "Some Aerodynamic Effects of Headshape Variation at Mach Number 2.44," Ballistic Research Laboratories Memorandum Report 838, October 1954. (AD 57748)*

21. *E. R. Dickinson, "Some Aerodynamic Effects of Varying the Body Length and Head Length of a Spinning Projectile," Ballistic Research Laboratories Memorandum Report 1664, July 1965. (AD 469897)*

22. *E. R. Dickinson, "The Effect of Boattailing on the Drag Coefficient of Cone-Cylinder Projectiles at Supersonic Velocities," Ballistic Research Laboratories Memorandum Report 842, November 1954. (AD 57769)*

23. *B. G. Karpov, "The Effect of Various Boattail Shapes on Base Pressure and Other Aerodynamic Characteristics of a 7-Caliber Long Body of Revolution at M = 1.70," Ballistic Research Laboratories Report 1295, August 1965. (AD 474352)*

Figure 13 compares the theoretical and experimental[9] effects of leading edge bluntness (méplatting) on secant-ogive noses at subsonic, transonic and supersonic speeds.

In Figures 14 through 24, the present theory and experimental results are compared for a number of different physical sizes and types of ordnance projectiles. The agreement is generally quite satisfactory for a program designed to give quick engineering estimates of drag. Figure 25 shows the standard deviation (1σ) of the MC DRAG program, as determined by comparison with a large volume of free flight data, plotted against Mach number. The standard deviation is about 6% in C_{D_o} at subsonic speeds, grows to a maximum of 11% at $M_\infty = 0.95$, and levels off to a 3% error at supersonic speeds. The largest errors at transonic speeds occur for boattailed projectiles, and this is believed to be related to the lack of any good similarity parameter for correlating transonic boattail effects.

IX. USER'S GUIDE FOR THE MC DRAG COMPUTER PROGRAM

The MC DRAG program* is designed to provide quick and reasonably accurate engineering estimates of the drag of ordnance projectiles, without the requirement of formal training in aerodynamics on the part of the user. The program input has been simplified to a single input card read per case, and the required projectile dimensions are readily obtained either from an assembly drawing or from measurements easily made in the shop. Although no computer program can be made foolproof, checks and warning prints have been included, to advise the unwary user that the program is being pushed beyond its limits of applicability.

The single input card, illustrated in Sketch 4, contains the following data:

* A listing of the FORTRAN IV program, MC DRAG is given in the Appendix.

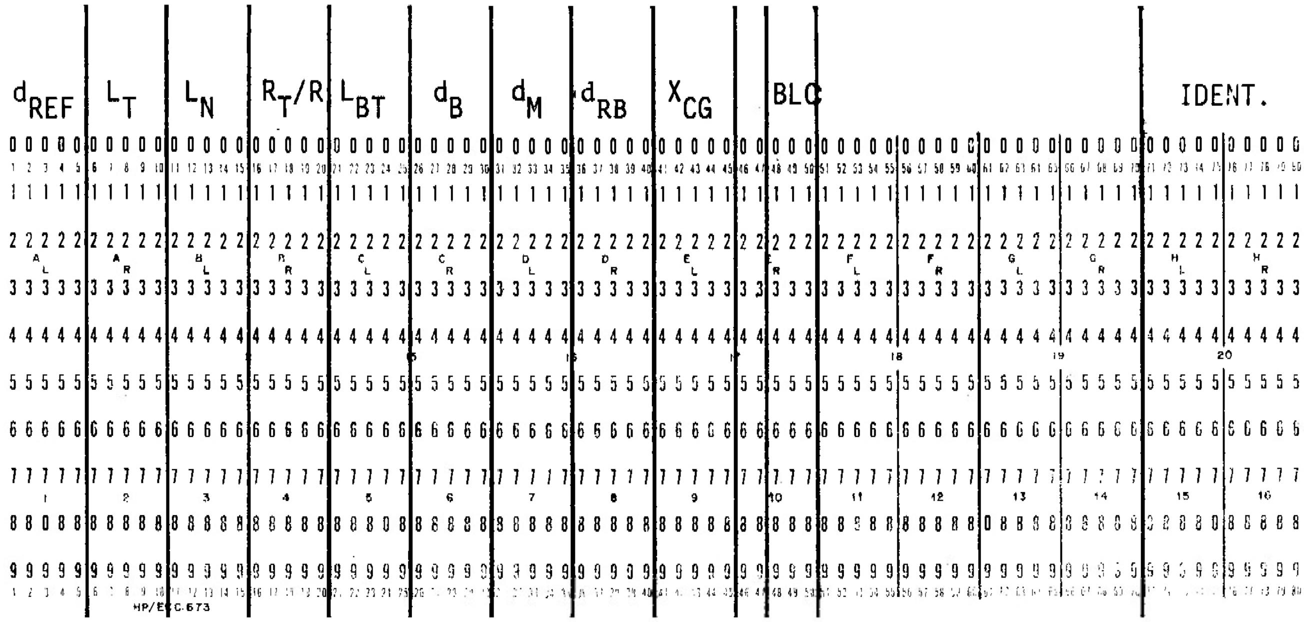

Sketch 4. Illustrated MC DRAG Program Input

COL	QUANTITY	FORTRAN FORMAT	COMMENTS
1-5	d_{REF}	F5.3	Reference diameter (mm)
6-10	L_T	↓	Projectile total length (calibers)
11-15	L_N	↓	Nose length (calibers)
16-20	R_T/R	↓	Headshape parameter
21-25	L_{BT}	↓	Boattail length (calibers)
26-30	d_B	↓	Base diameter (calibers)
31-35	d_M	↓	Méplat diameter (calibers)
36-40	d_{RB}	↓	Rotating band diameter (calibers)
41-45	X_{CG}	↓	Center of gravity (calibers from nose)
46-47	——	BLANK	
48-50	BLC	A3	Boundary layer option (L/T or T/T)
51-70	——	BLANK	
71-80	CODE	A10	Alphanumeric identification

The rules for obtaining projectile dimensions from drawings will be illustrated, using three specific examples. For projectile designs other than those usually encountered, some judgment must be exercised. For example, a pure cone projectile would require that $L_T = L_N$, $R_T/R = 0$, $L_{BT} = 0$, $d_B = 1$, $d_M = 0$ (providing the cone is pointed), $d_{RB} = 1$. A projectile with a hemispherical nose can be run, with $L_n = \frac{1}{2}$ and $R_T/R = 1$, but this nose is too blunt for the program to give reasonable accuracy, and a warning print will follow the output to so advise the user. The MC DRAG program does not recognize the existence of a sub-caliber, or boom, tail, and the boom of such a design should be ignored in assigning total length. In general, nose lengths shorter than one caliber will produce warning prints, as will boattails longer than 1.5 calibers, or base diameters less than 0.65 caliber.

The first example projectile is an experimental low-drag small arms bullet, the 5.56mm BRL-1 design (see Figure 16). The bullet drawing shape, as given in reference 24, is reproduced below. The reference

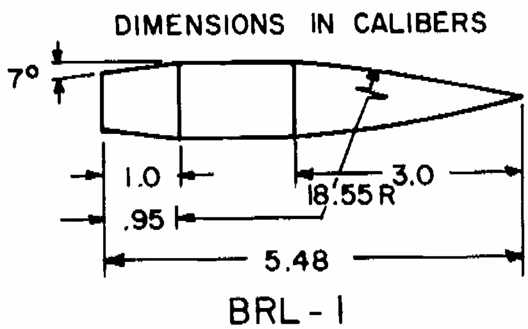

Sketch 5. Projectile Drawing, 5.56mm, BRL-1

---

24. *W. F. Braun, "Aerodynamic Data for Small Arms Projectiles," Ballistic Research Laboratories Report 1630, January 1973. (AD 909757L)*

diameter is given as 0.224 inch, or 5.69mm. Total length is 5.48 calibers, nose length is 3.0 calibers. The headshape parameter, R_T/R, is found as follows. The ogive generating radius is given as 18.55 calibers. The radius R_T is the radius of a tangent ogive nose having the same length. For a pointed tangent ogive nose of length $\hat{L}_N$, the length and radius are related by the following equation:

$$R_T = (\hat{L}_N)^2 + \tfrac{1}{4} \tag{20}$$

If the actual nose of the projectile is not sharply pointed, extend it to a point (a graphic extension is sufficiently accurate for this purpose), and determine the length, $\hat{L}_N$, that the nose would have if it were sharply pointed. Then compute R_T from Equation 20, and divide by R from the drawing to get R_T/R.

NOTE: For an actual tangent ogive nose, $R = R_T$, hence $R_T/R = 1$. For a conical nose, $R \rightarrow \infty$, and $R_T/R \approx 0$. Hence no calculation is required for either of these nose shapes.

For the pointed BRL-1 design, $\hat{L}_N = L_N = 3.0$ calibers, and $R_T = (3.0)^2 + \tfrac{1}{4} = 9.25$ calibers. Hence, $R_T/R = 9.25/18.55 = 0.50$. This is essentially a minimum drag nose shape at supersonic speeds.

The boattail length for BRL-1 is 1.0 caliber, and the boattail angle is 7 degrees; hence, the base diameter is 0.754 caliber. The nose is essentially sharp-pointed, thus mēplat diameter is zero. There is no rotating band, so $d_{RB} = 1.0$. The center of gravity is 3.34 calibers from the nose and this value is included in the input as identification information. Since the reference diameter is much smaller than 20mm, and the projectile surface is relatively smooth, the expected (verified by shadowgraphs) boundary layer option is L/T: laminar nose, turbulent afterbody.

The output of the MC DRAG program for the BRL-1 projectile is shown as Figure 26. The total drag coefficient and component parts are tabulated for pre-selected Mach numbers. The last column is the program estimate of the ratio of base pressure to free stream static pressure. (Note: the computer program uses the notation CDBND for $C_{D_{RB}}$). The comparison of MC DRAG with experimental results for BRL-1 is shown in Figure 16.

The second example projectile is a scale model of a Minuteman re-entry stage vehicle, which was fired through the BRL Transonic Range for aerodynamic data determination. The model drawing shape as given in reference 25 is reproduced below.

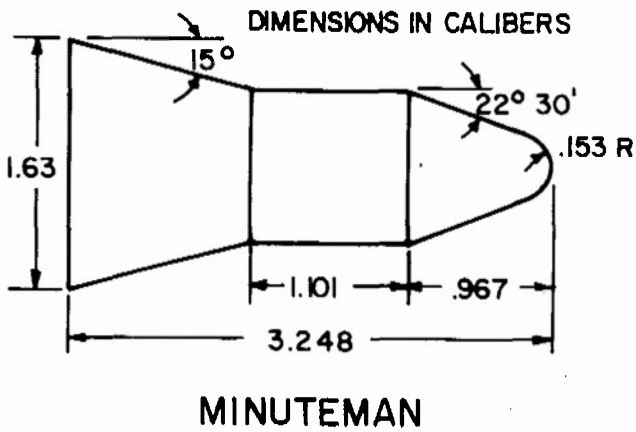

Sketch 6. Projectile Drawing, 55mm Minuteman Model

NOTE: The base diameter shown on the drawing in reference 25 is incorrect; the correct base diameter (Sketch 6) is obtained from the length and angle of the flare tail. The MC DRAG program user is advised to check all drawing dimensions for internal consistency, as a surprising number of errors have been found in report drawings.

The reference diameter of the Minuteman model is 55.6mm. Total length is 3.25 calibers, nose length is 0.967 caliber. The nose is conical, hence $R_T/R = 0$. The flare (boattail) length is 1.18 calibers, and the correct base diameter is 1.63 calibers. The nose has an inscribed hemispherical tip, which is not recognized by MC DRAG . The proper procedure for this case is to extend the actual nose out to the leading edge, and determine the méplat diameter of the extended nose. The geometry of the extension for the Minuteman model is shown in Sketch 7.

---

25. *E. D. Boyer, "Free Flight Range Tests of a Minuteman Re-Entry Stage Model," Ballistic Research Laboratories Memorandum Report 1346, May 1961. (AD 326744)*

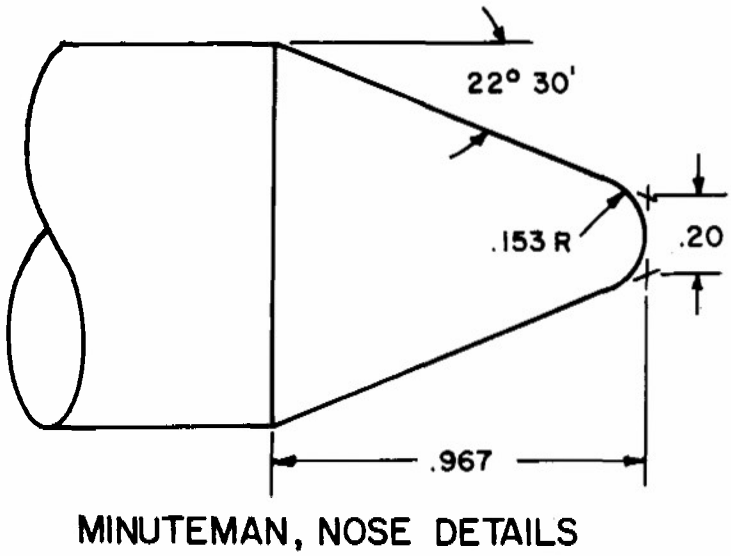

Sketch 7. Minuteman Model, Nose Detail

The effective méplat diameter of the Minuteman model nose is 0.20 caliber. There is no rotating band, so d_{RB} = 1.0, and the center of gravity is 1.76 calibers from the nose. Since reference diameter is larger than 20mm, choose T/T for the boundary layer option.

The output of MC DRAG for the Minuteman model is shown as Figure 34. The program warning print tells us that this nose is really too blunt for an accurate drag estimate with MC DRAG . In addition, the predicted ratio of base pressure to free stream static pressure shows negative values at high supersonic speeds, which is physically erroneous, and suggests that this flare is probably too steep for the program. Nevertheless, the comparison between MC DRAG and experiment, shown in Figure 21, indicates better accuracy than would be expected for a design that violates the program limitations.

The last example projectile is the 155mm long-range artillery shell, M549. The projectile drawing shape is shown in Sketch 8[26].

---

26. *R. Kline, W. R. Herrmann and V. Oskay. "A Determination of the Aerodynamic Coefficients of the 155mm, M549 Projectile," Picatinny Arsenal Technical Report 4764, November 1974. (AD B002073L)*

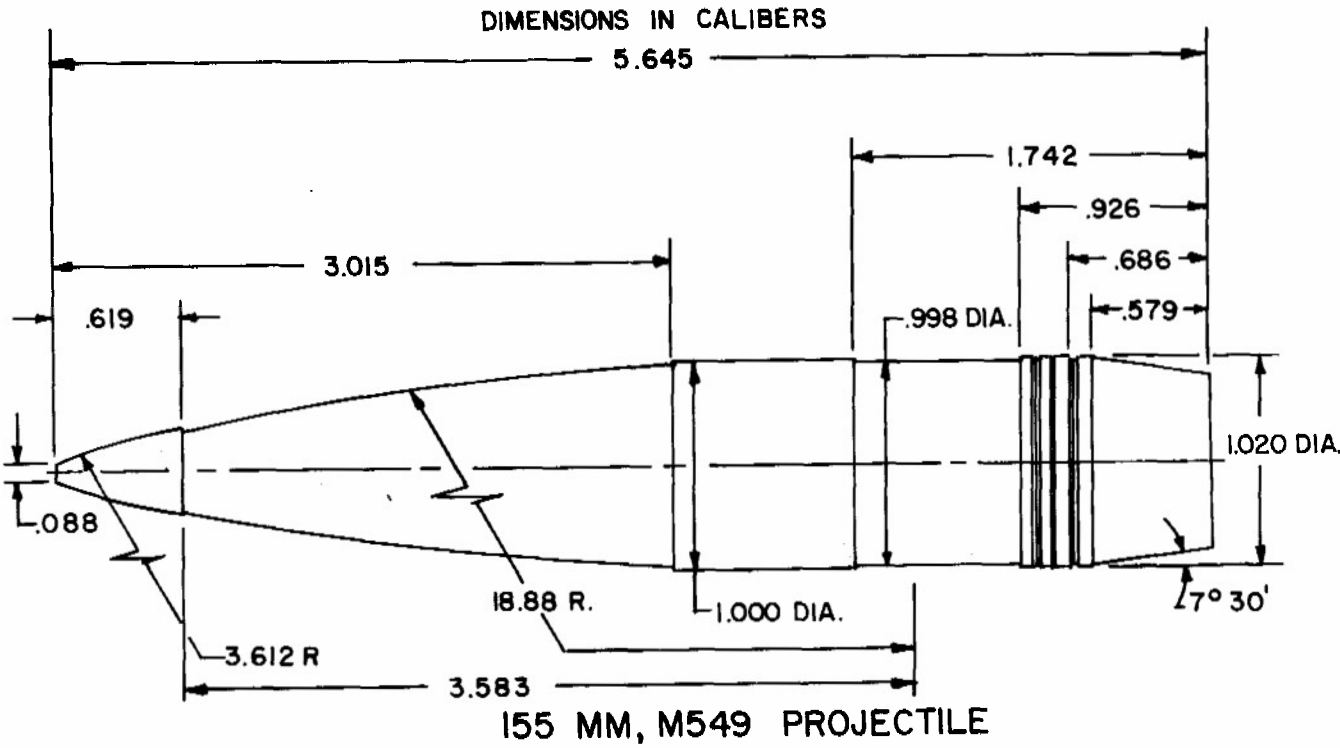

Sketch 8. Projectile Drawing, 155mm M549 Projectile

The reference diameter is 155mm, total length is 5.65 calibers, nose length is 3.01 calibers. If the ogive nose is extended to a sharp point (ignore the fuze for headshape parameter calculation), a pointed nose length, $\hat{L}_N$, of 3.03 calibers is obtained. Thus R_T = 9.43 calibers, and R_T/R = 0.50. The boattail length is .58 caliber, base diameter is 0.848 caliber, and the mêplat diameter is given as 0.09 caliber. The rotating band diameter is 1.02 calibers and the center of gravity is 3.53 calibers from the nose. The proper boundary layer option is again T/T.

The MC DRAG output for the M549 projectile is shown as Figure 28. The comparison of MC DRAG with experiment for this projectile is shown in Figure 23.

X. CONCLUSIONS

Comparisons of MC DRAG with experimental data have demonstrated the ability of the program to estimate accurately the effects of systematic changes in projectile configuration. Additional comparisons of the program with alternative theoretical methods show MC DRAG to be as good as or better than the competitive methods for conventional projectiles. The limits of applicability of MC DRAG are believed to be wider than those of any competitive approach. The MC DRAG program estimates the drag coefficient of typical ordnance projectiles to within 3% error (1σ) at supersonic speeds, 11% error at transonic speeds, and 6% error at subsonic speeds.

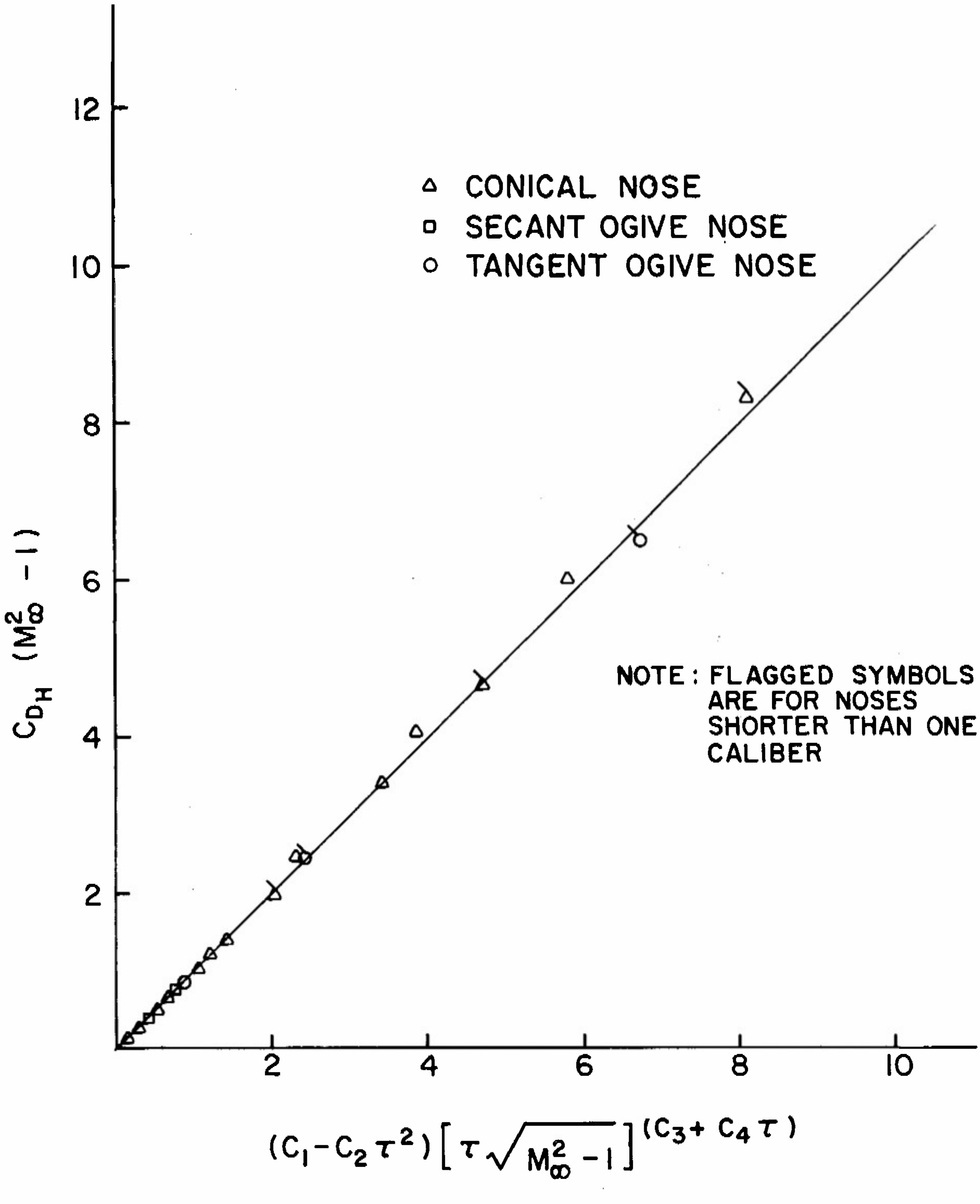

Figure 1. Correlation of Supersonic Head Drag Coefficients with Mach Number

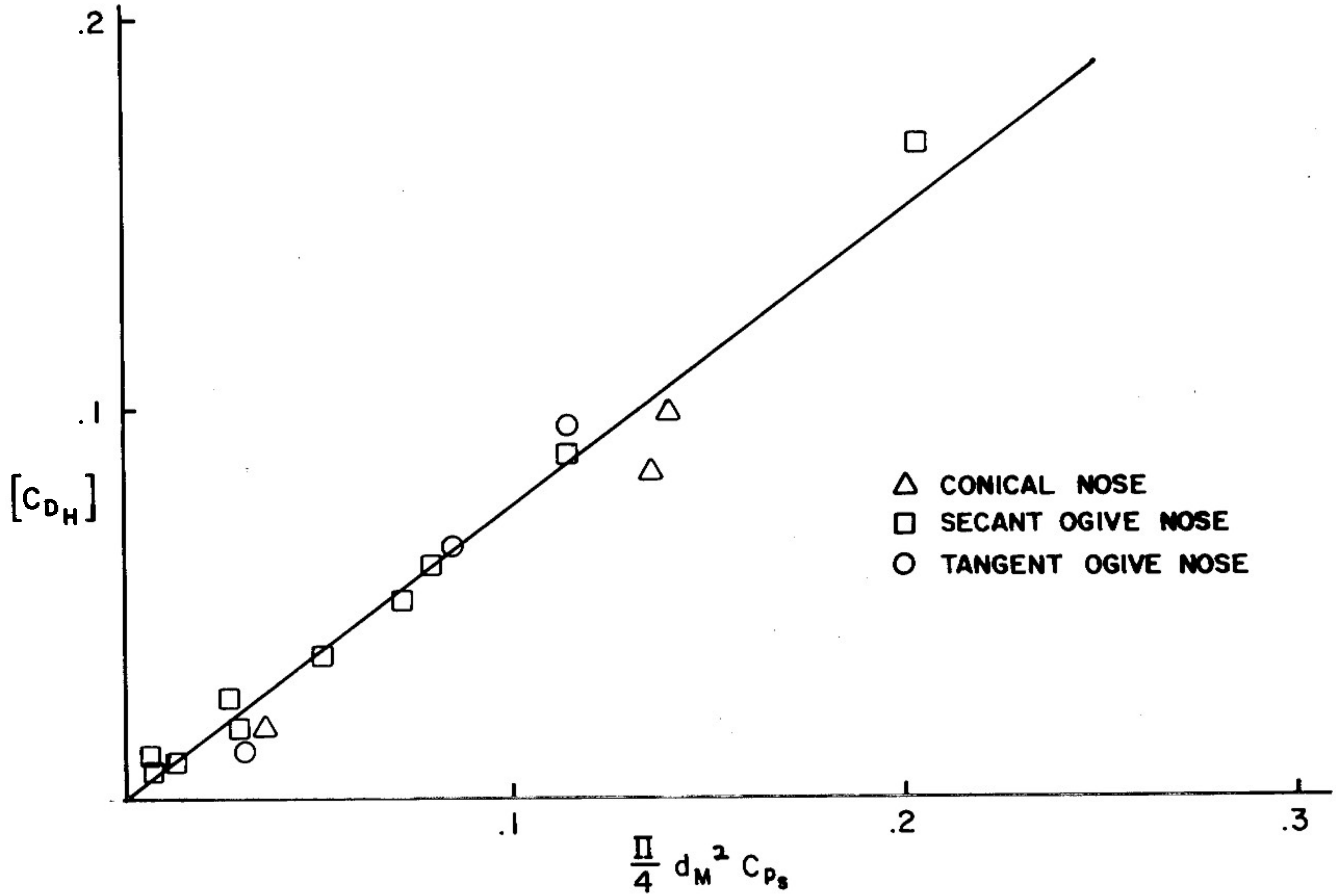

Figure 2. Correlation of Supersonic Méplat Drag Coefficients With Stagnation Pressure

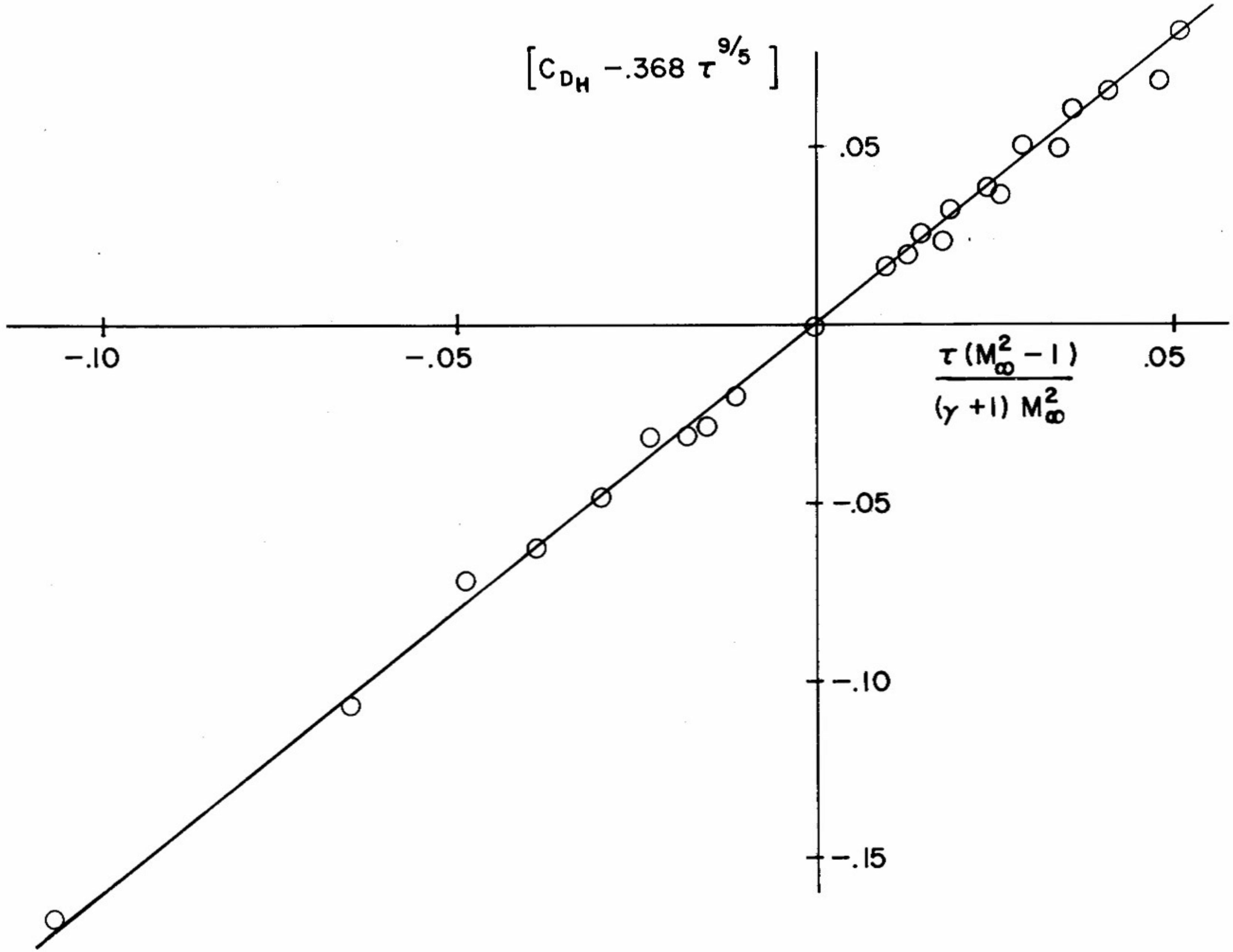

Figure 3. Correlation of Transonic Head Drag Coefficient With Thickness Ratio and Mach Number

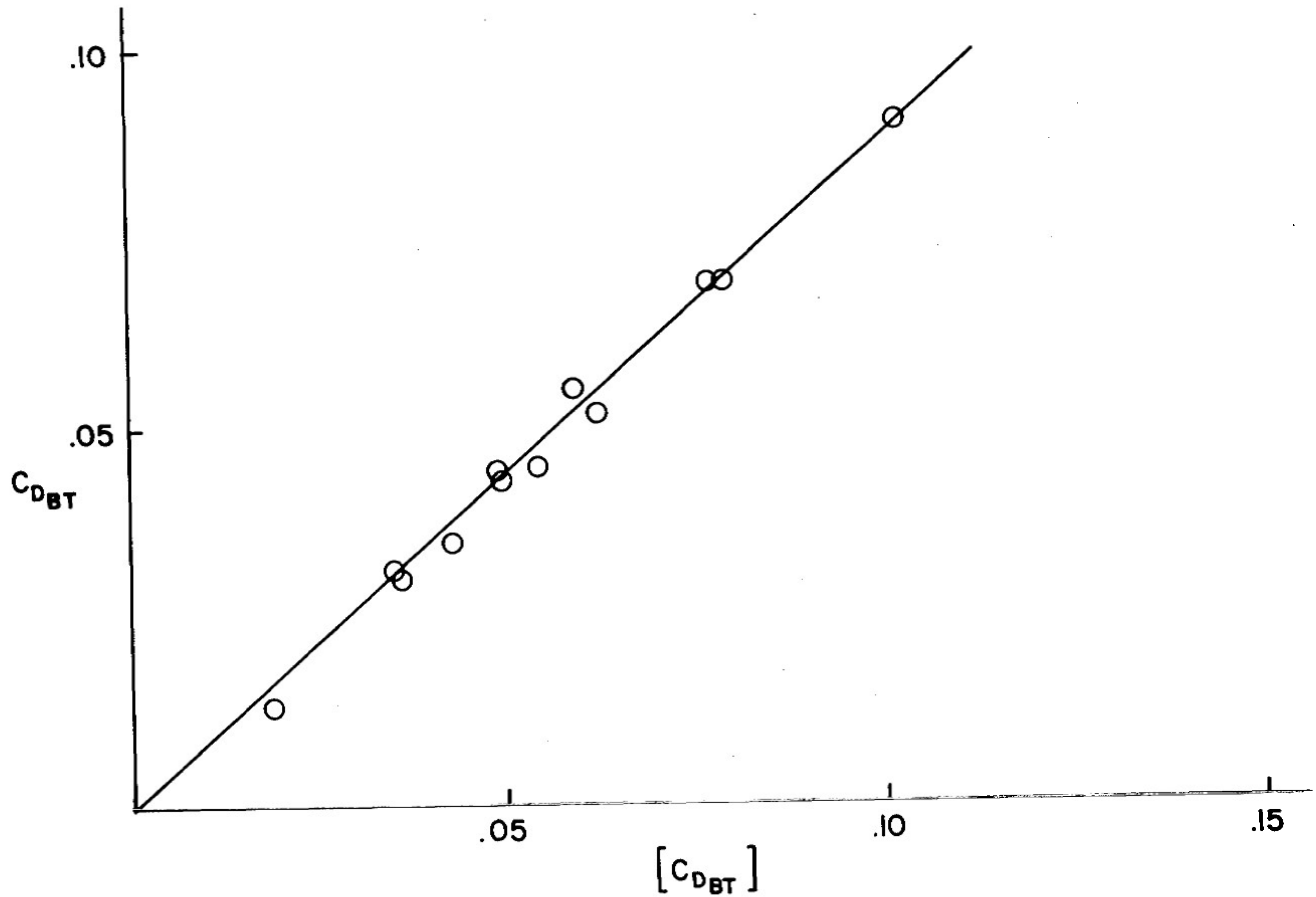

Figure 4. Correlation of Supersonic Boattail Drag Coefficient With the Similarity Parameter

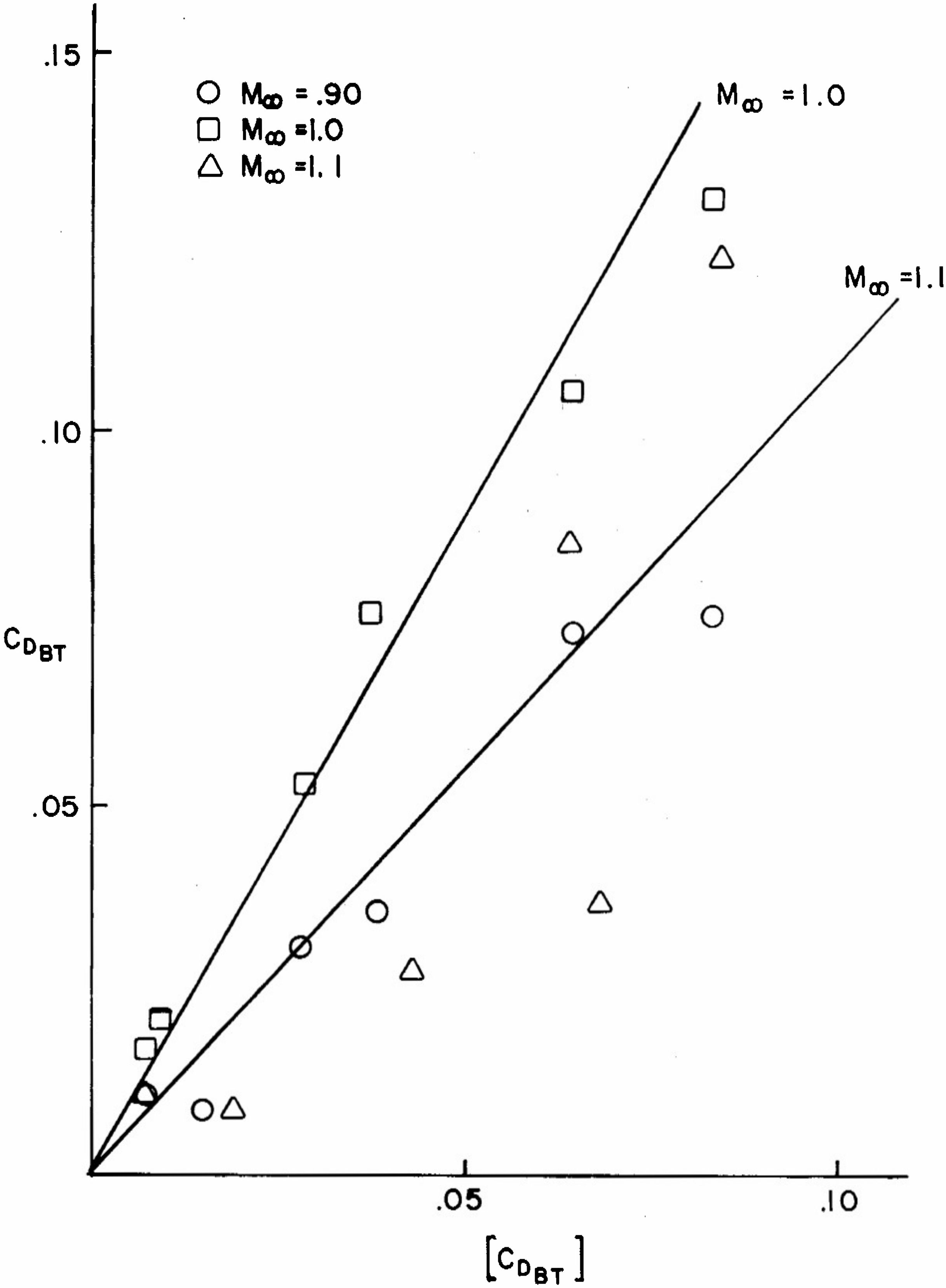

Figure 5. Correlation of Transonic Boattail Drag Coefficient With the Similarity Parameter

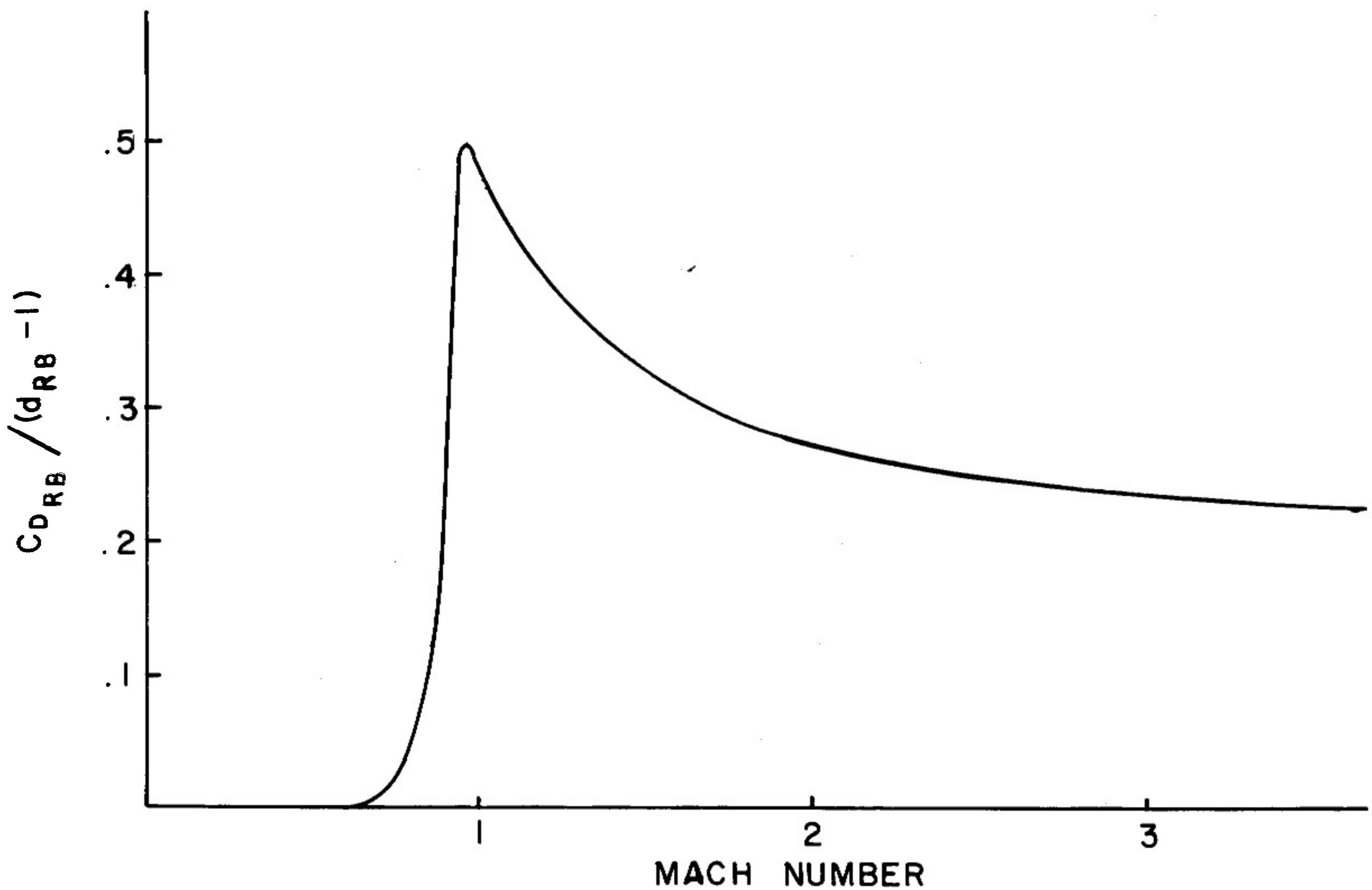

Figure 6. Rotating Band Drag Coefficient

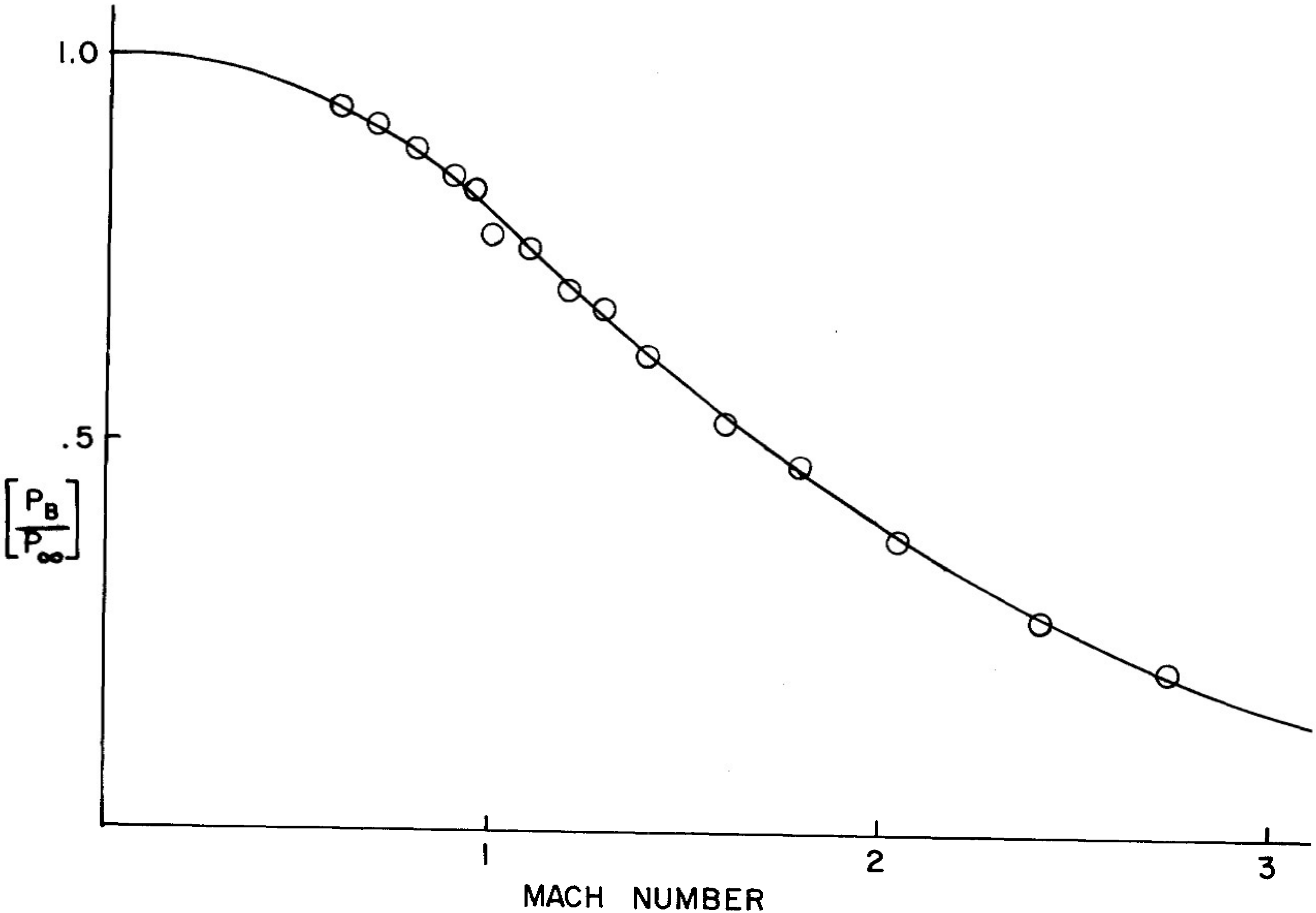

Figure 7. Correlation of Base Pressure Ratio With Mach Number

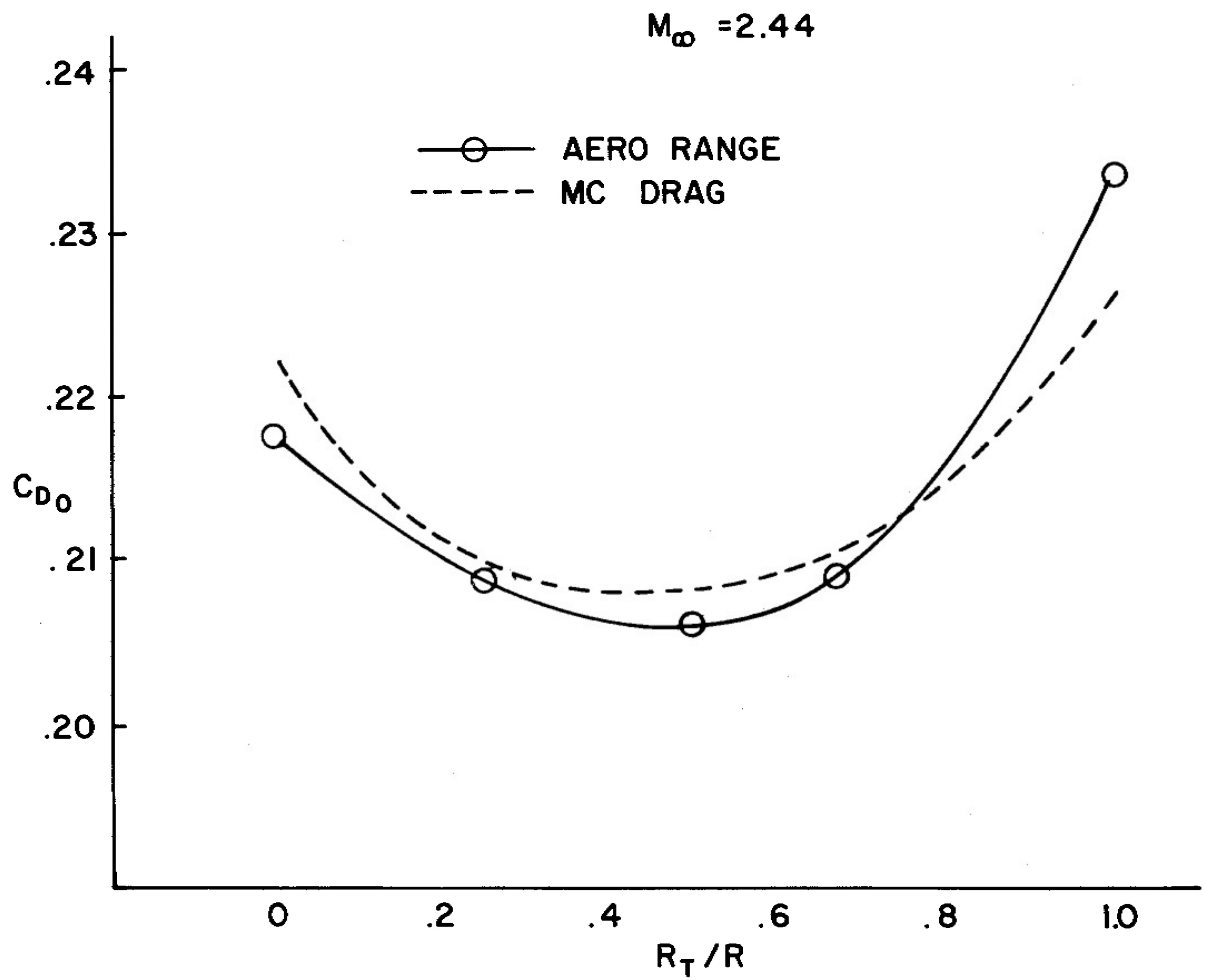

Figure 8. Effect of Headshape on Drag Coefficient

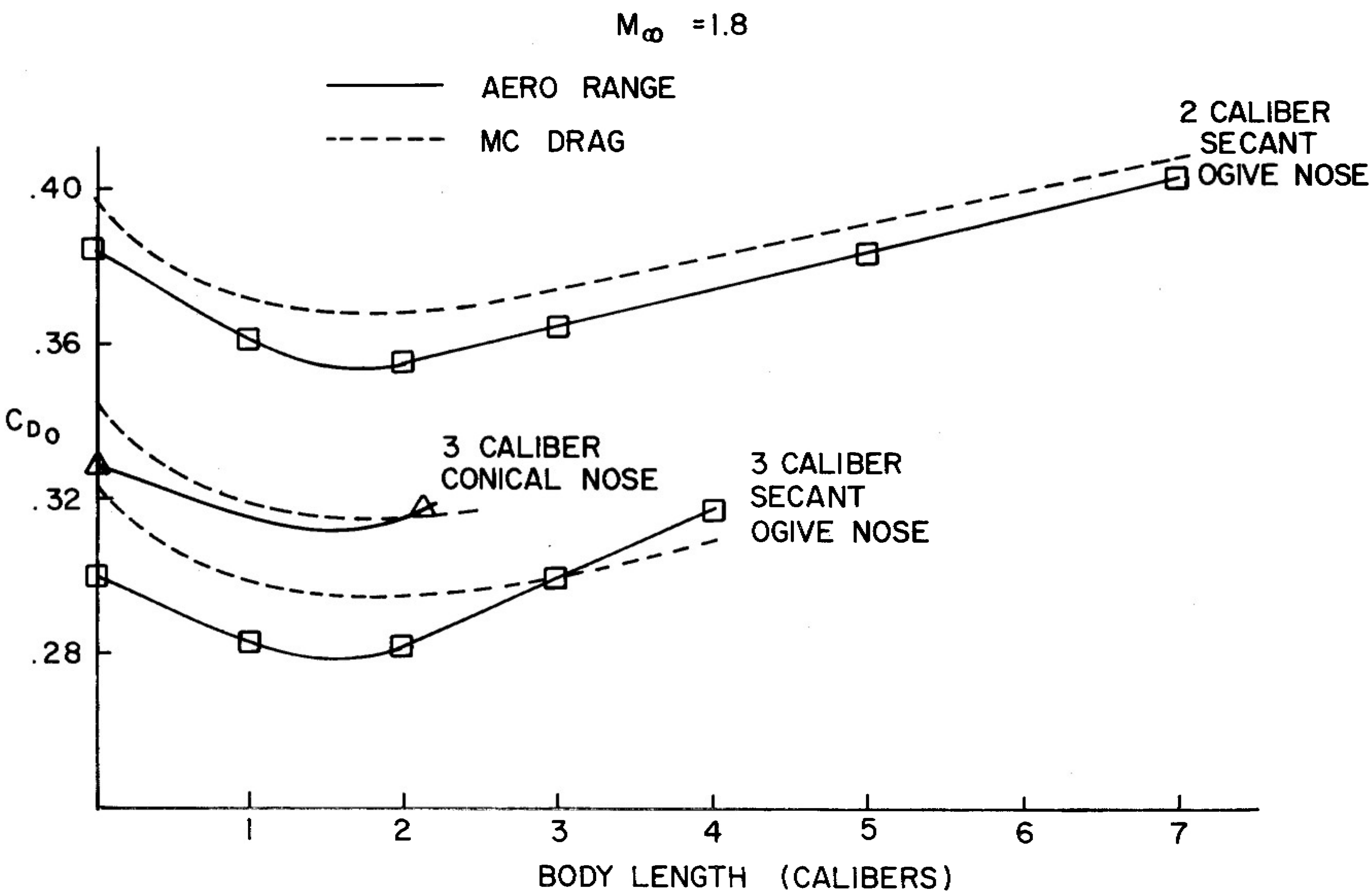

Figure 9. Effect of Afterbody Length on Drag Coefficient

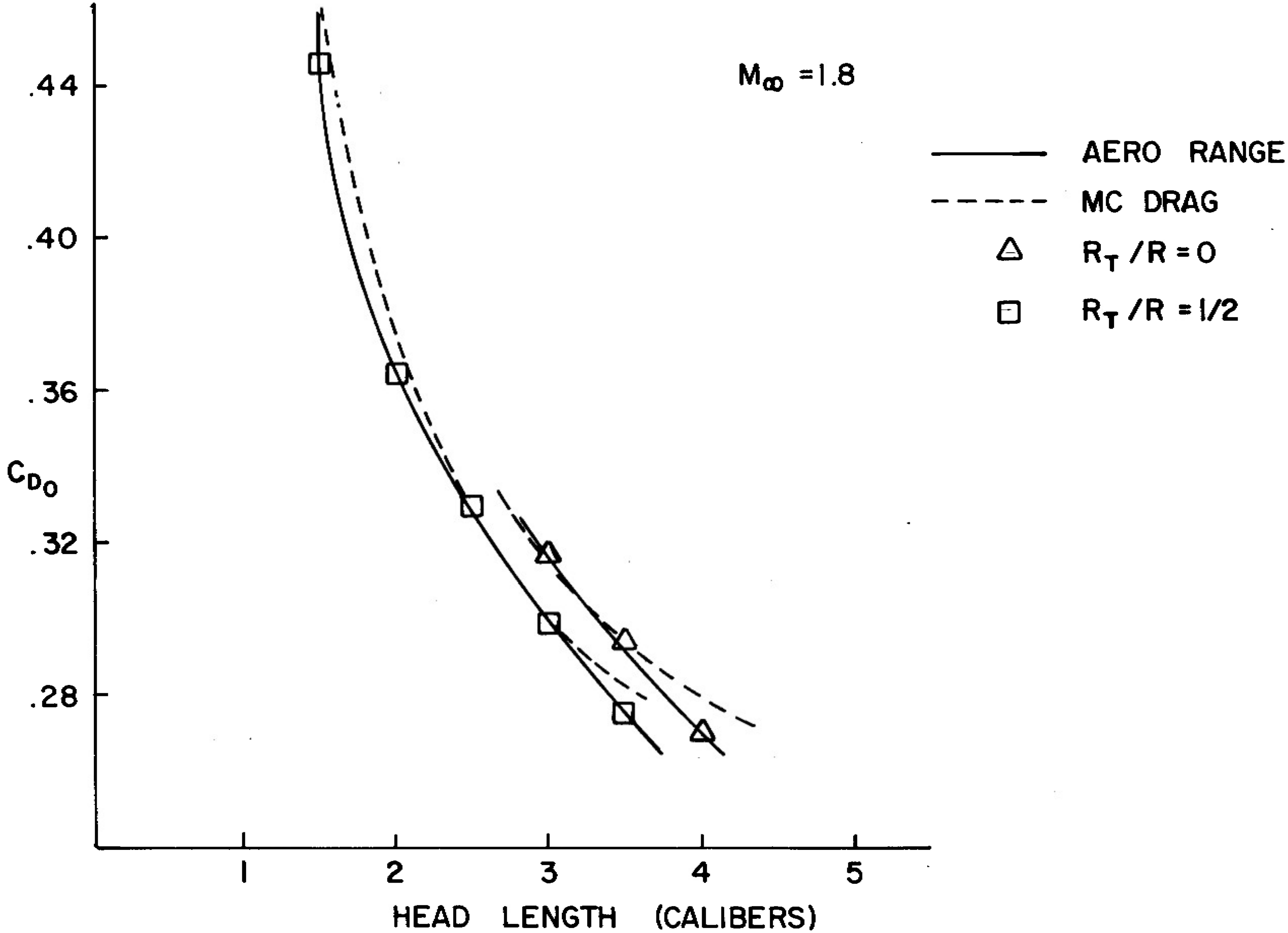

Figure 10. Effect of Head Length on Drag Coefficient

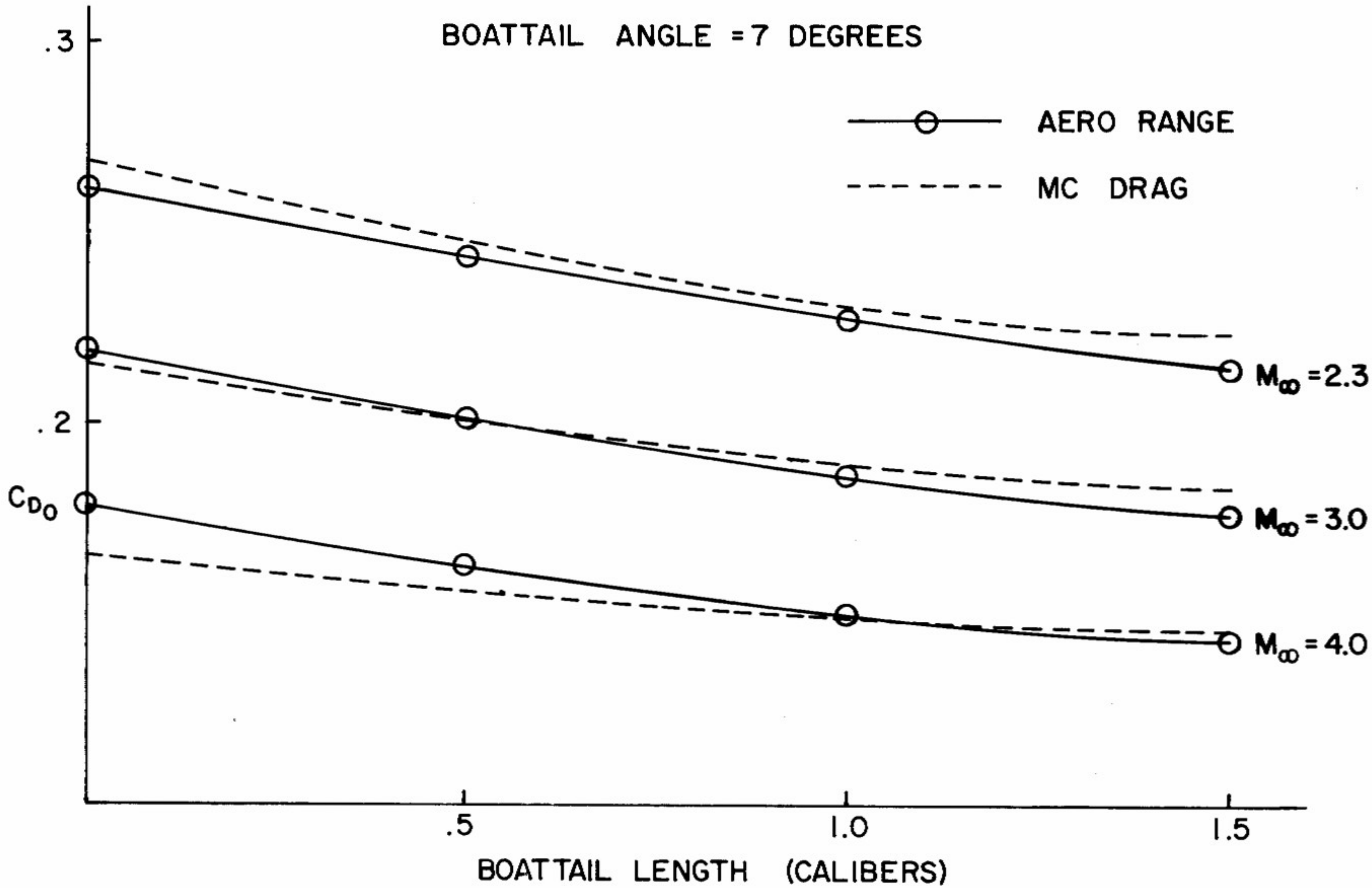

Figure 11. Effect of Boattail Length on Drag Coefficient

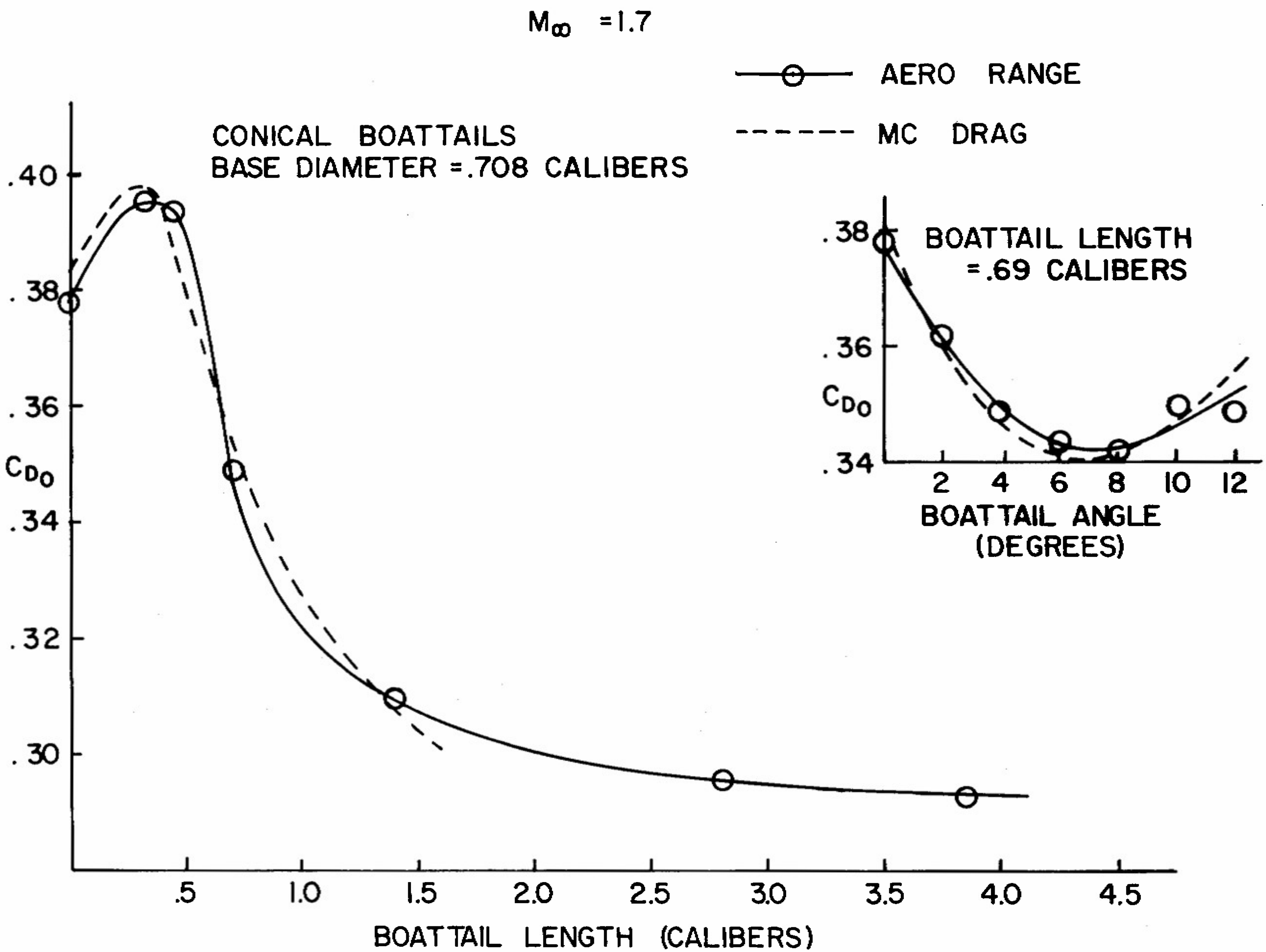

Figure 12. Effect of Boattail Length and Boattail Angle on Drag Coefficient

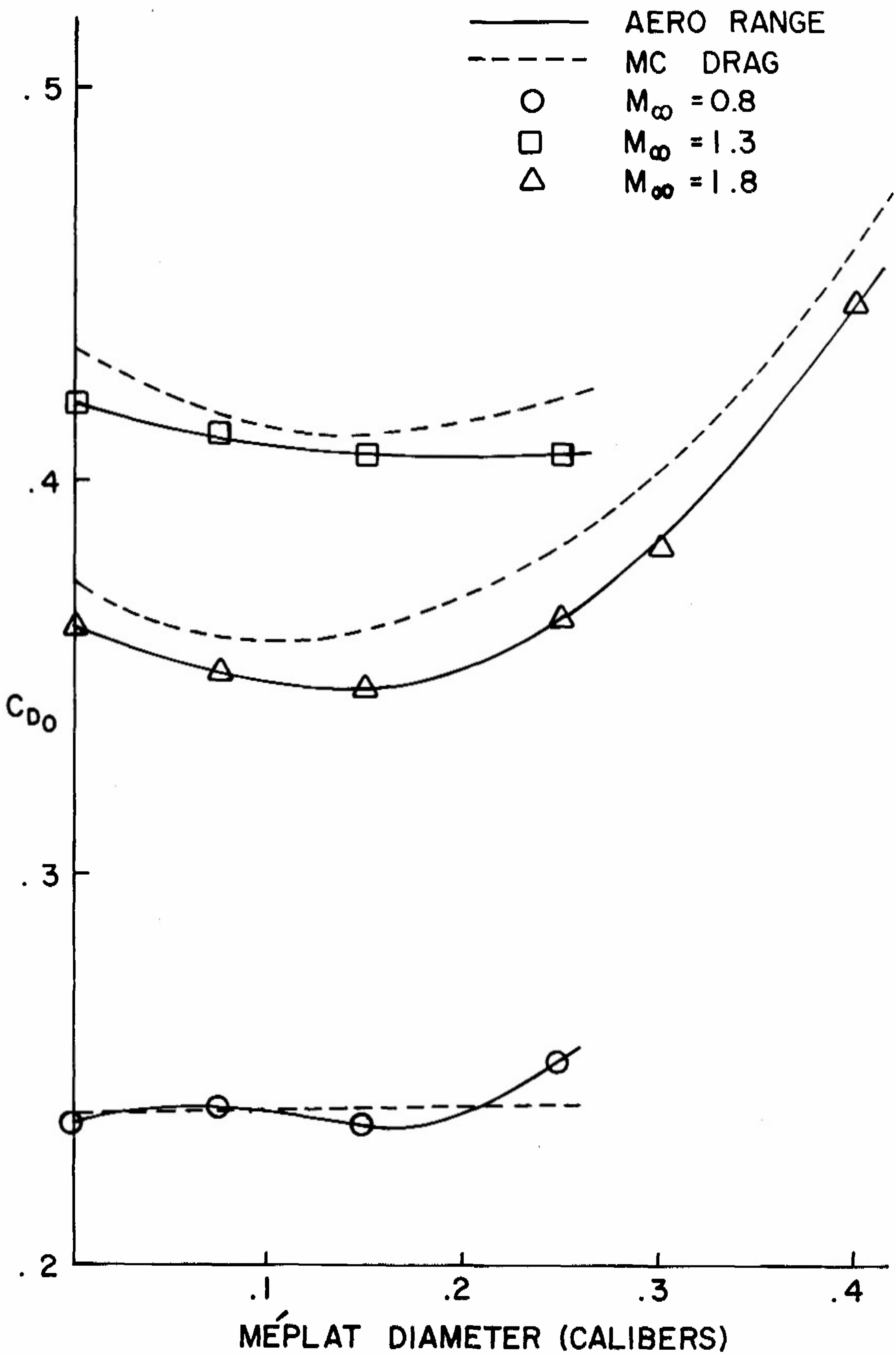

Figure 13. Effect of a Méplat on Drag Coefficient

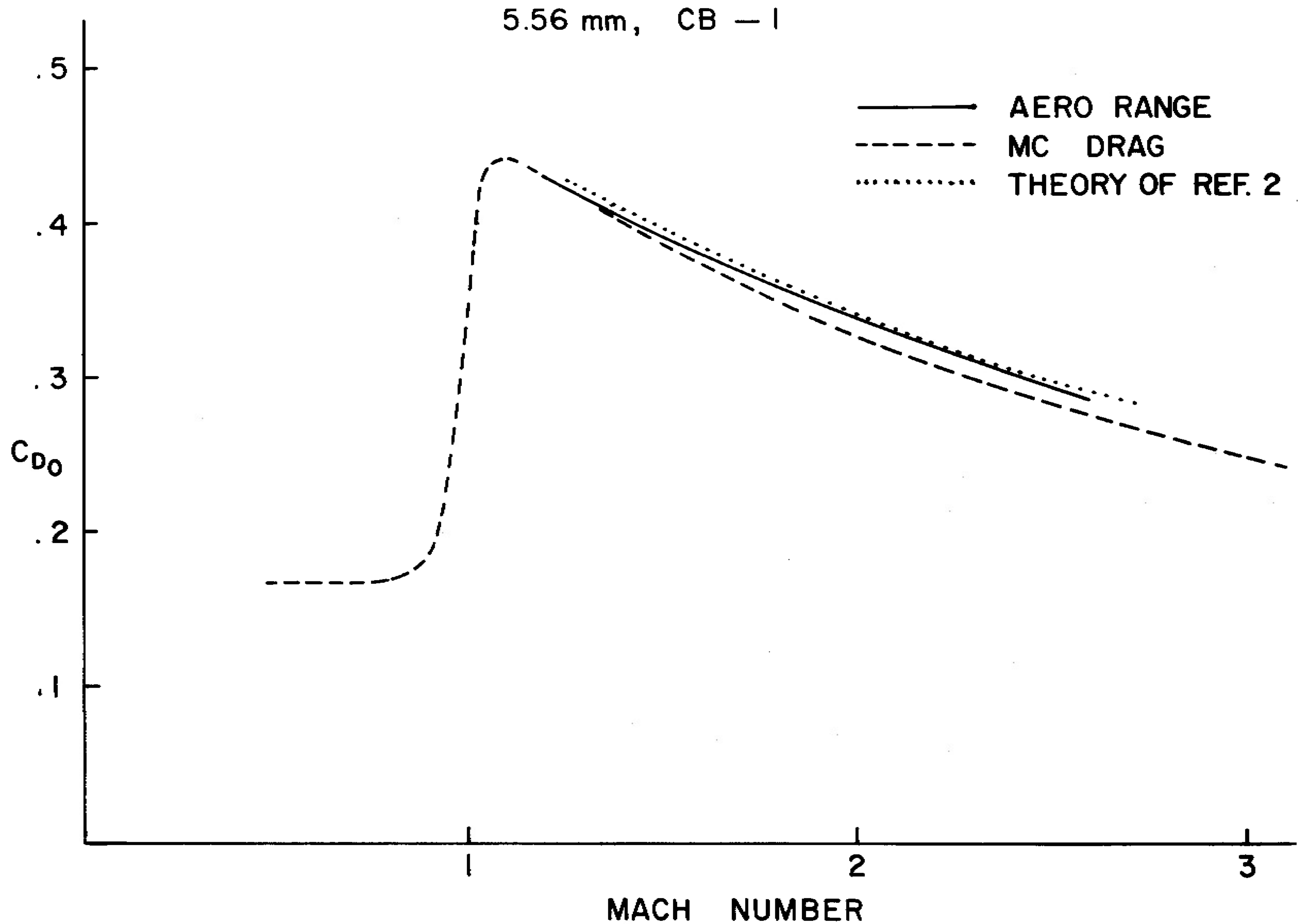

Figure 14. Drag Coefficient vs Mach Number, 5.56mm, CB-1

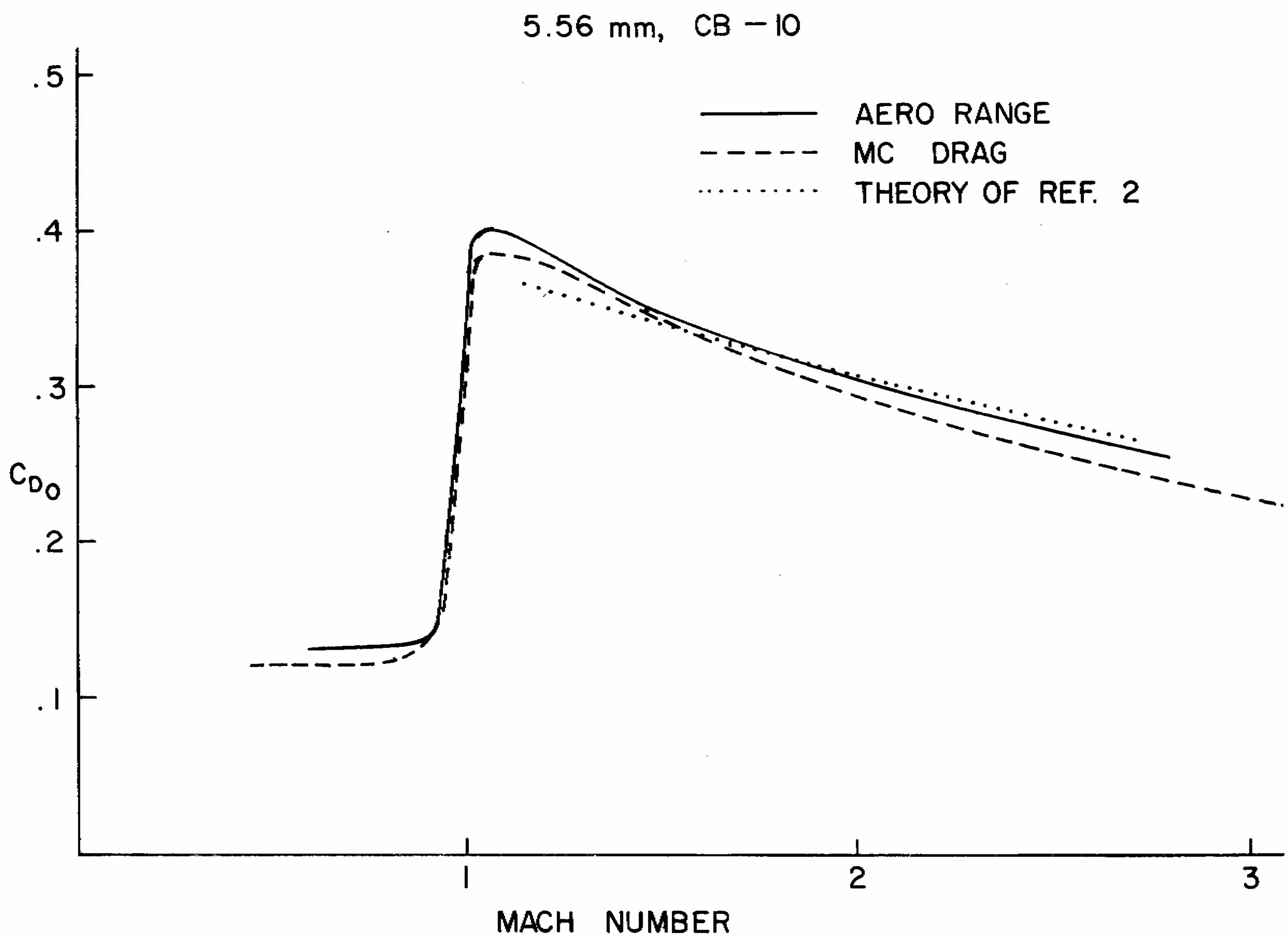

Figure 15. Drag Coefficient vs Mach Number, 5.56mm, CB-10

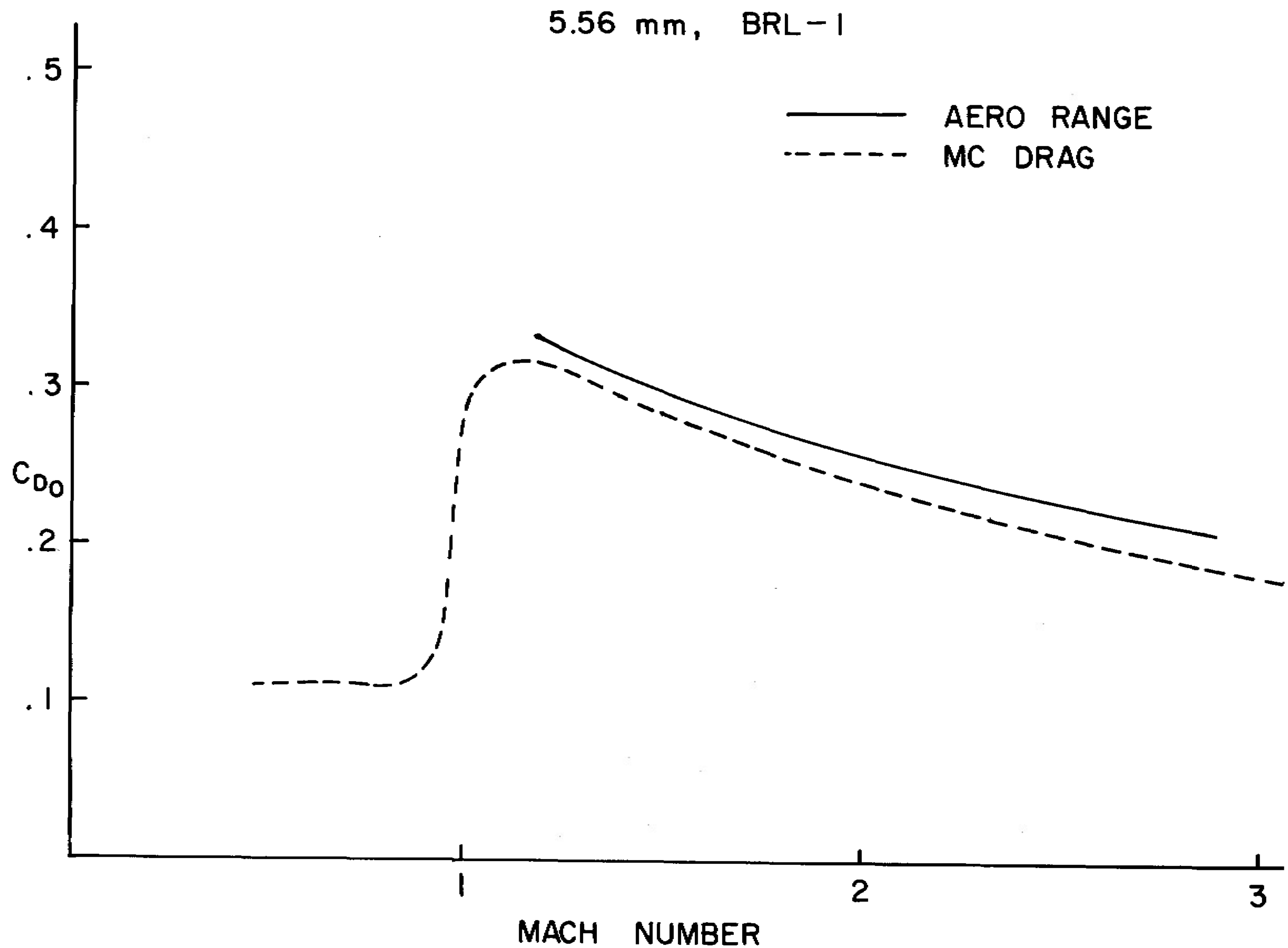

Figure 16. Drag Coefficient vs Mach Number, 5.56mm, BRL-1

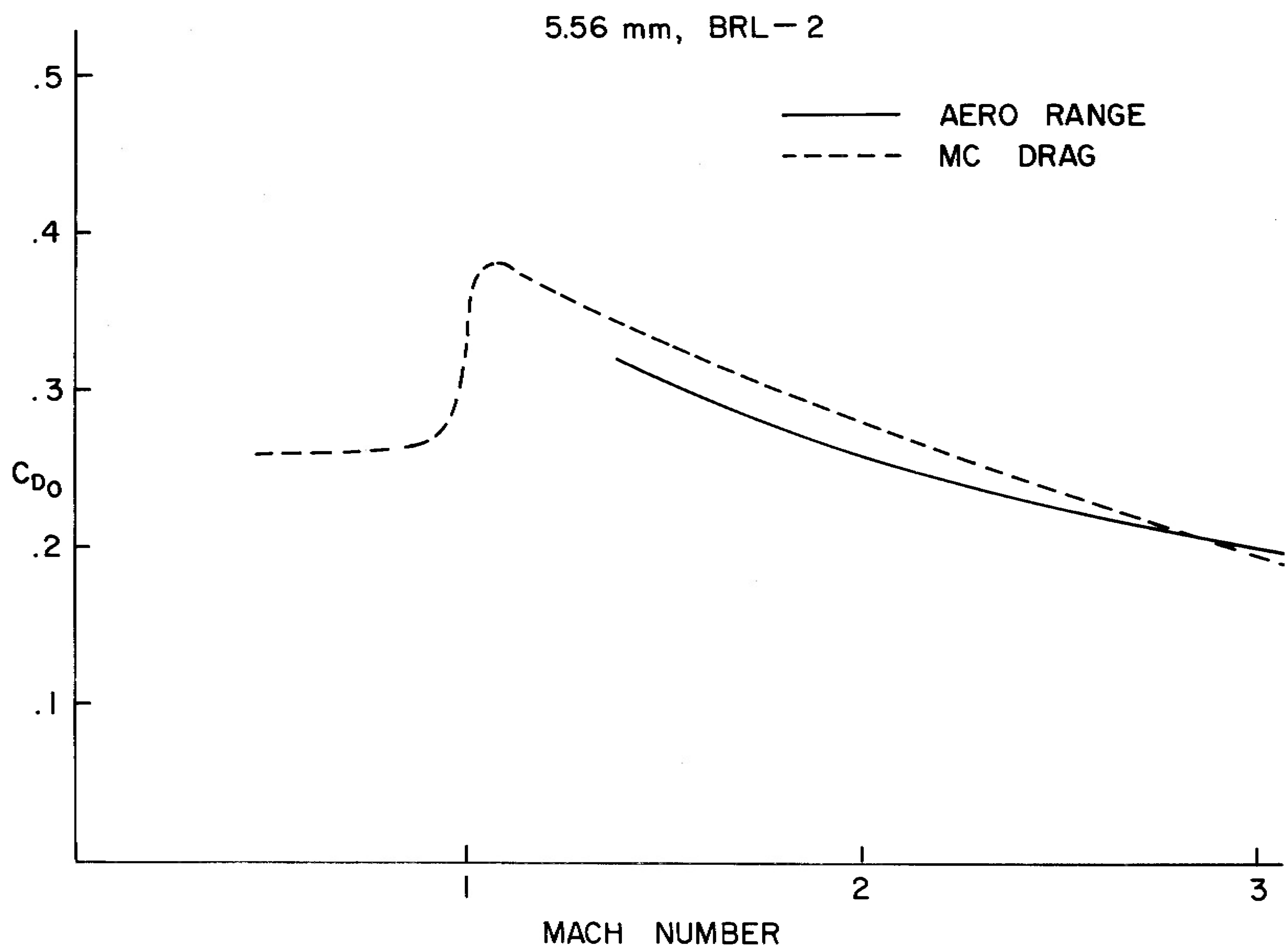

Figure 17. Drag Coefficient vs Mach Number, 5.56mm, BRL-2

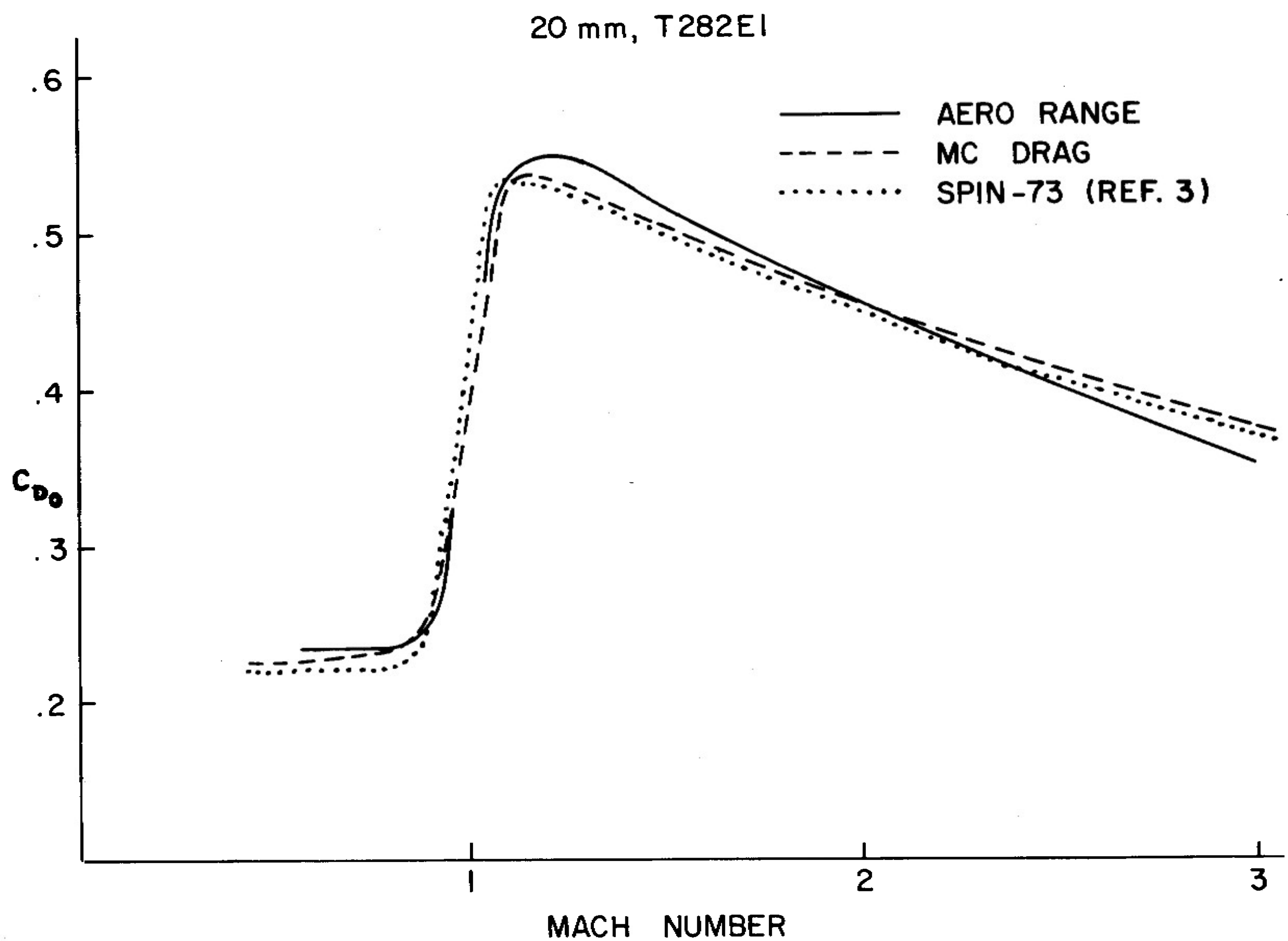

Figure 18. Drag Coefficient vs Mach Number, 20mm, T282E1

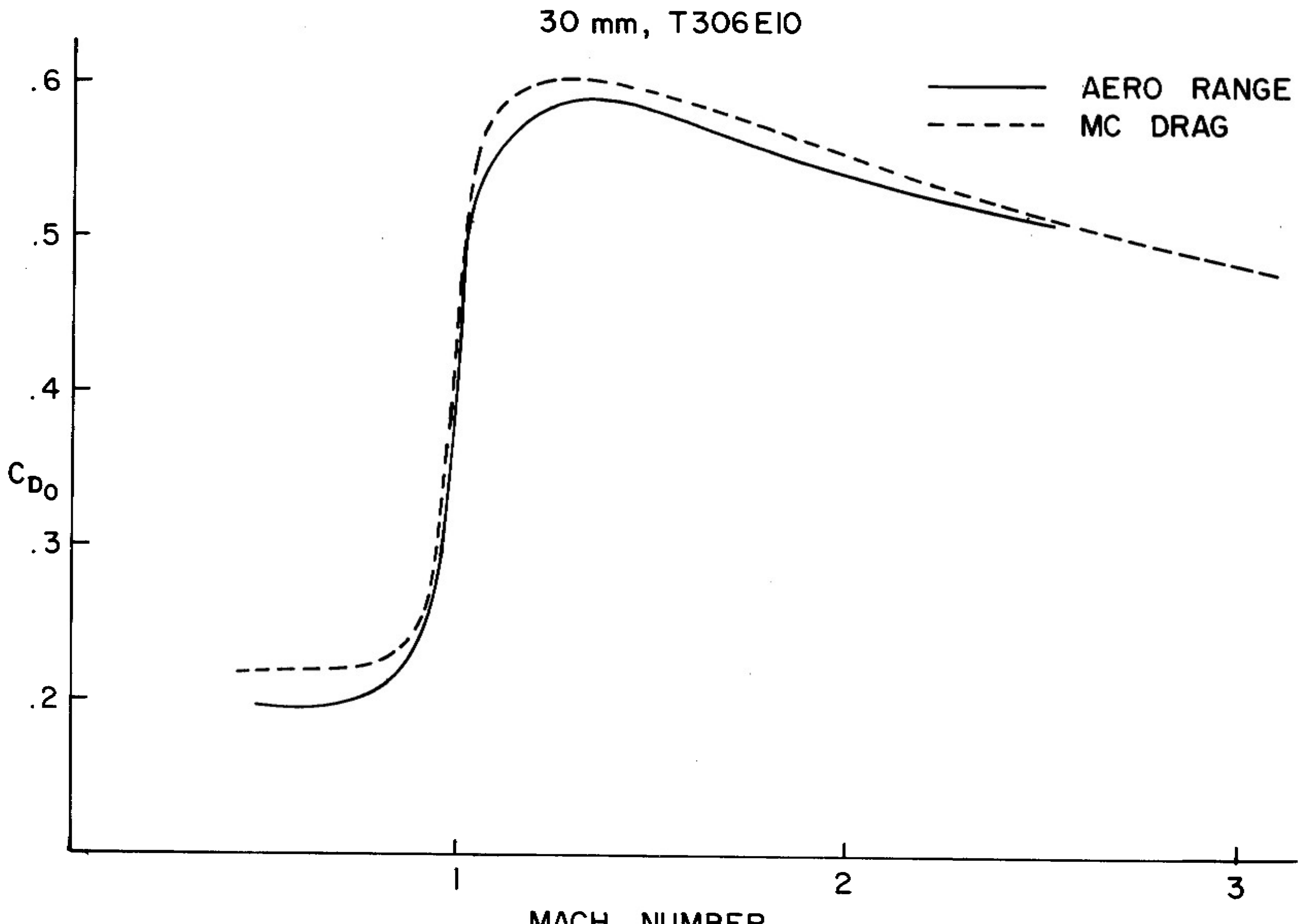

Figure 19. Drag Coefficient vs Mach Number, 30mm, T306E10

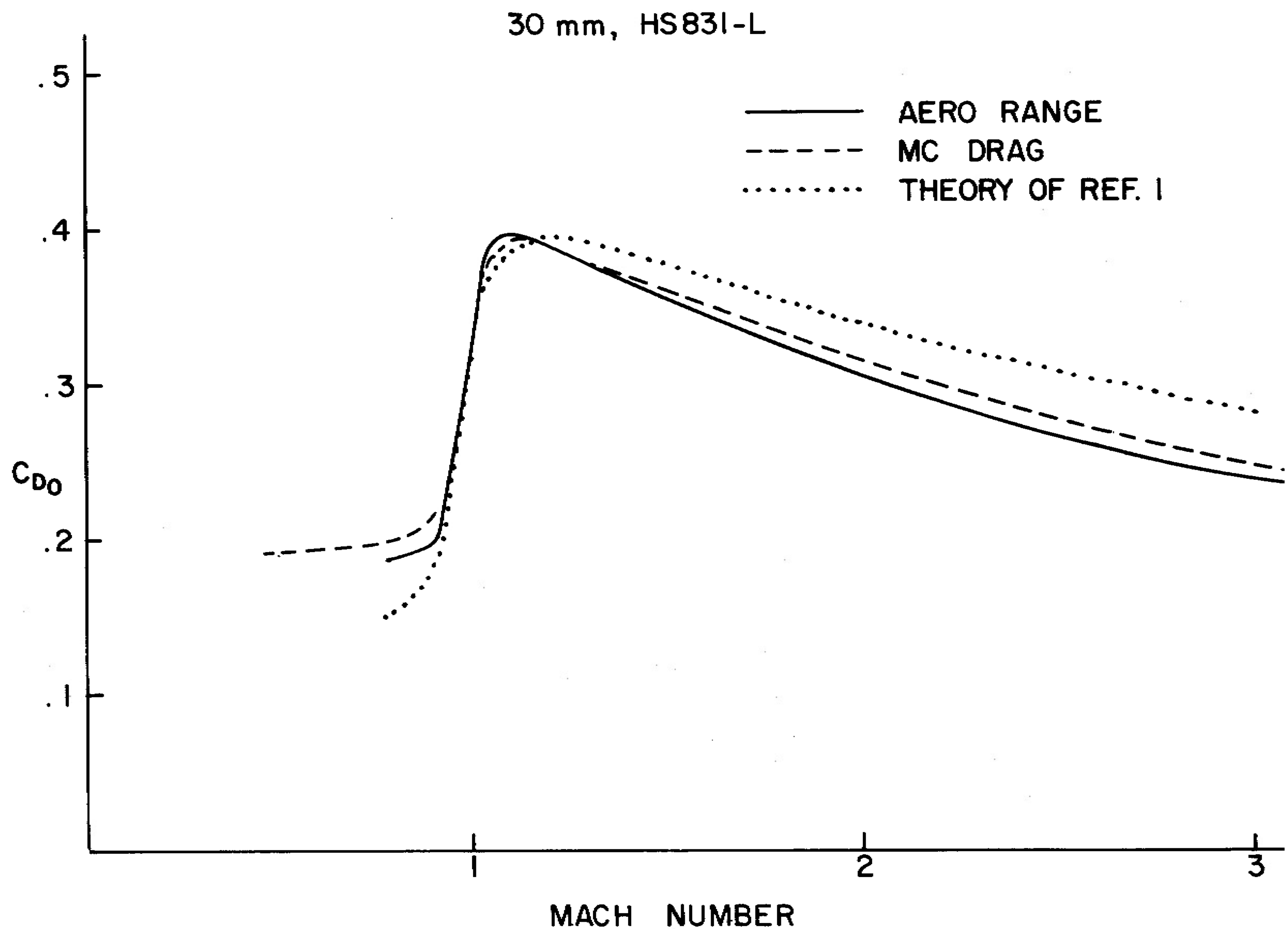

Figure 20. Drag Coefficient vs Mach Number, 30mm, HS831-L

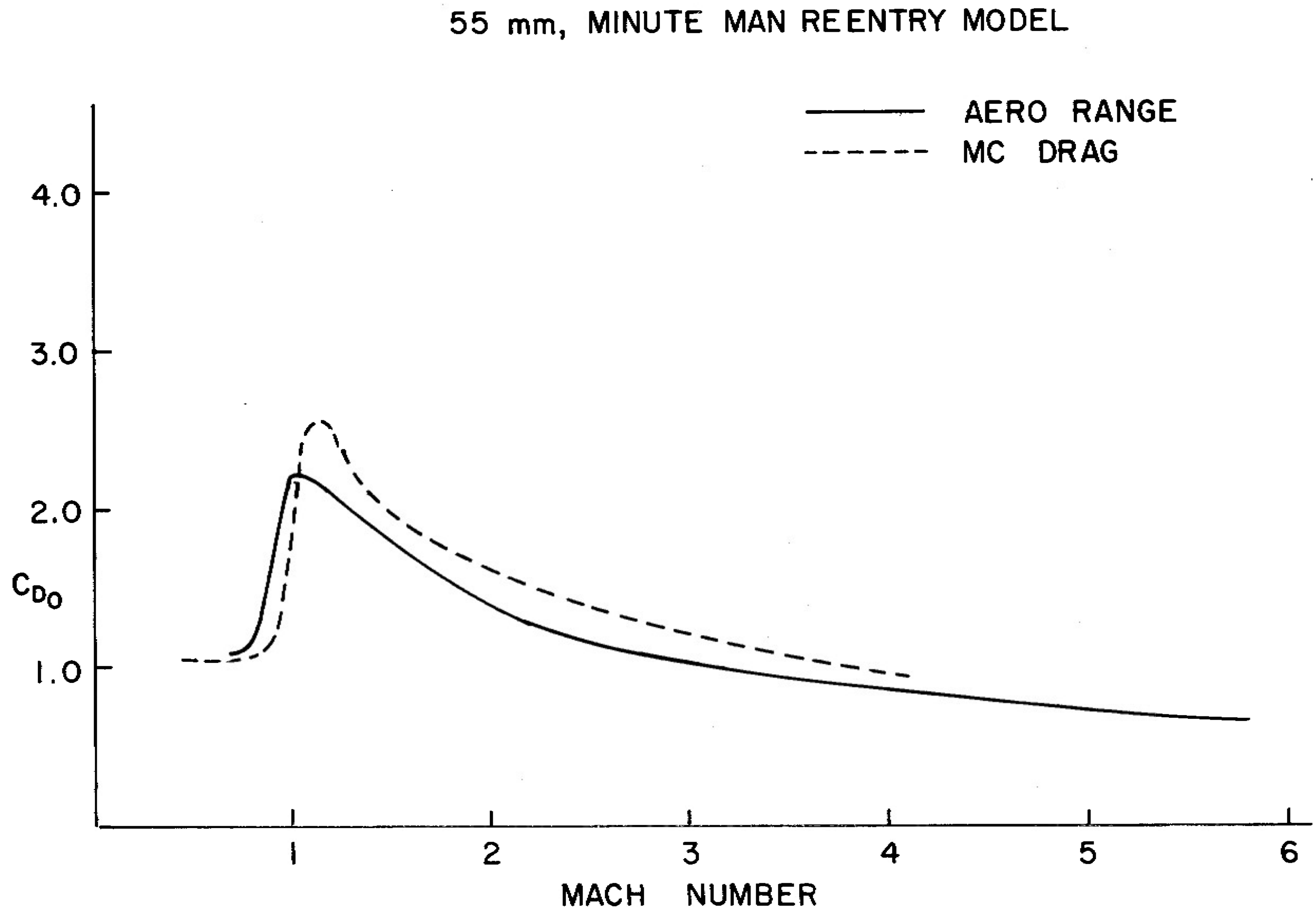

Figure 21. Drag Coefficient vs Mach Number, 55mm Minuteman Model

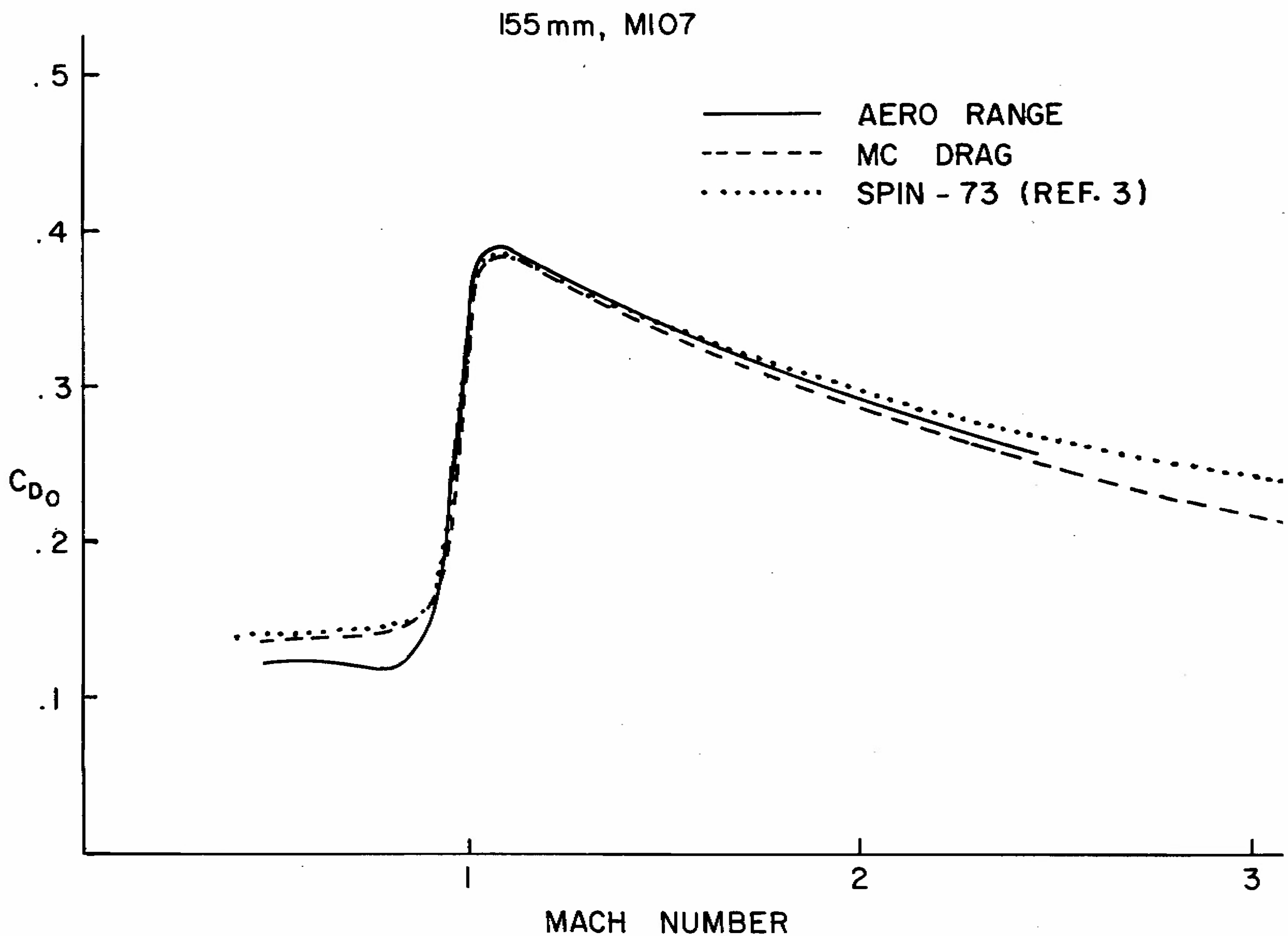

Figure 22. Drag Coefficient vs Mach Number, 155mm, M107

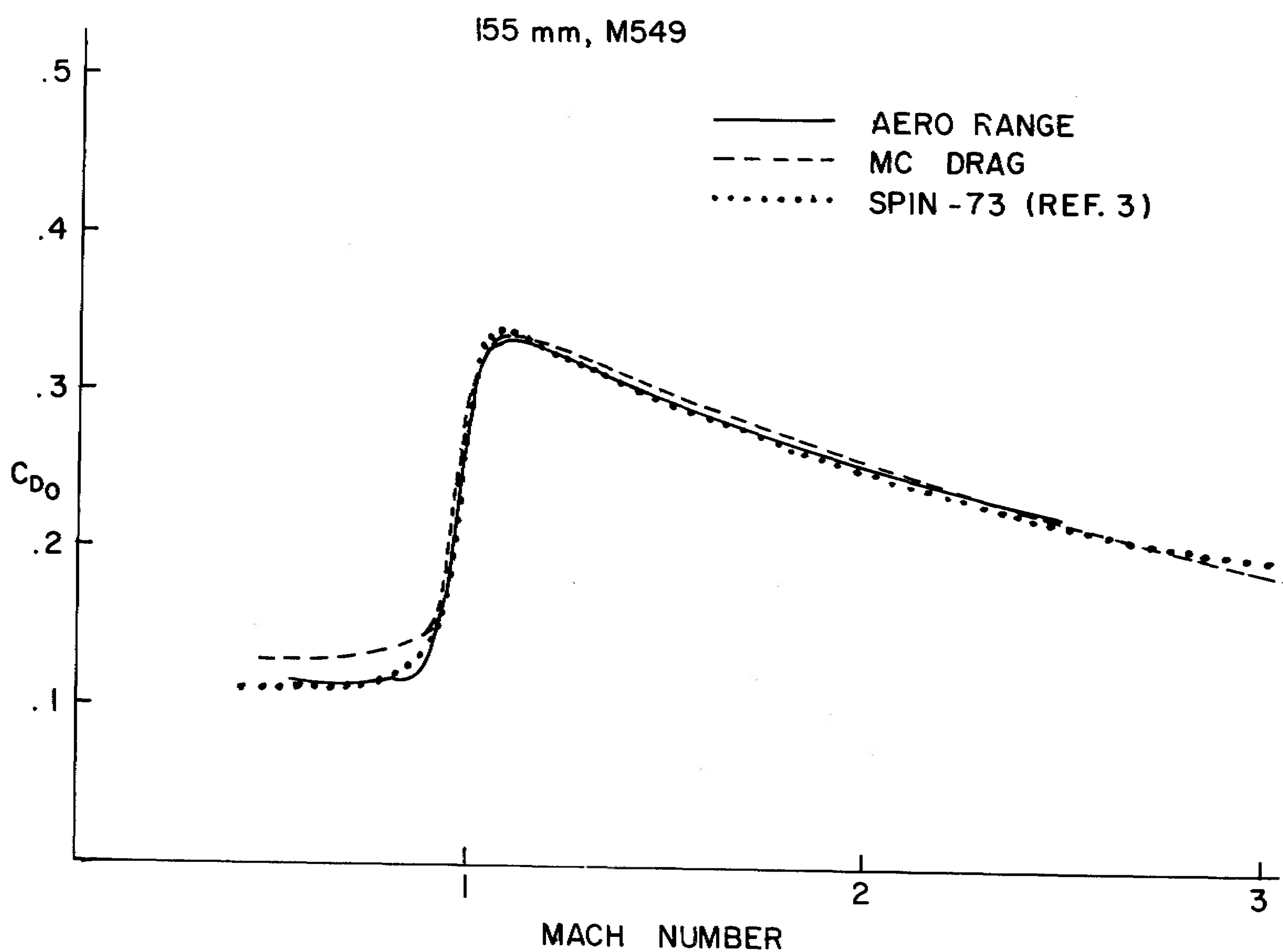

Figure 23. Drag Coefficient vs Mach Number, 155mm, M549

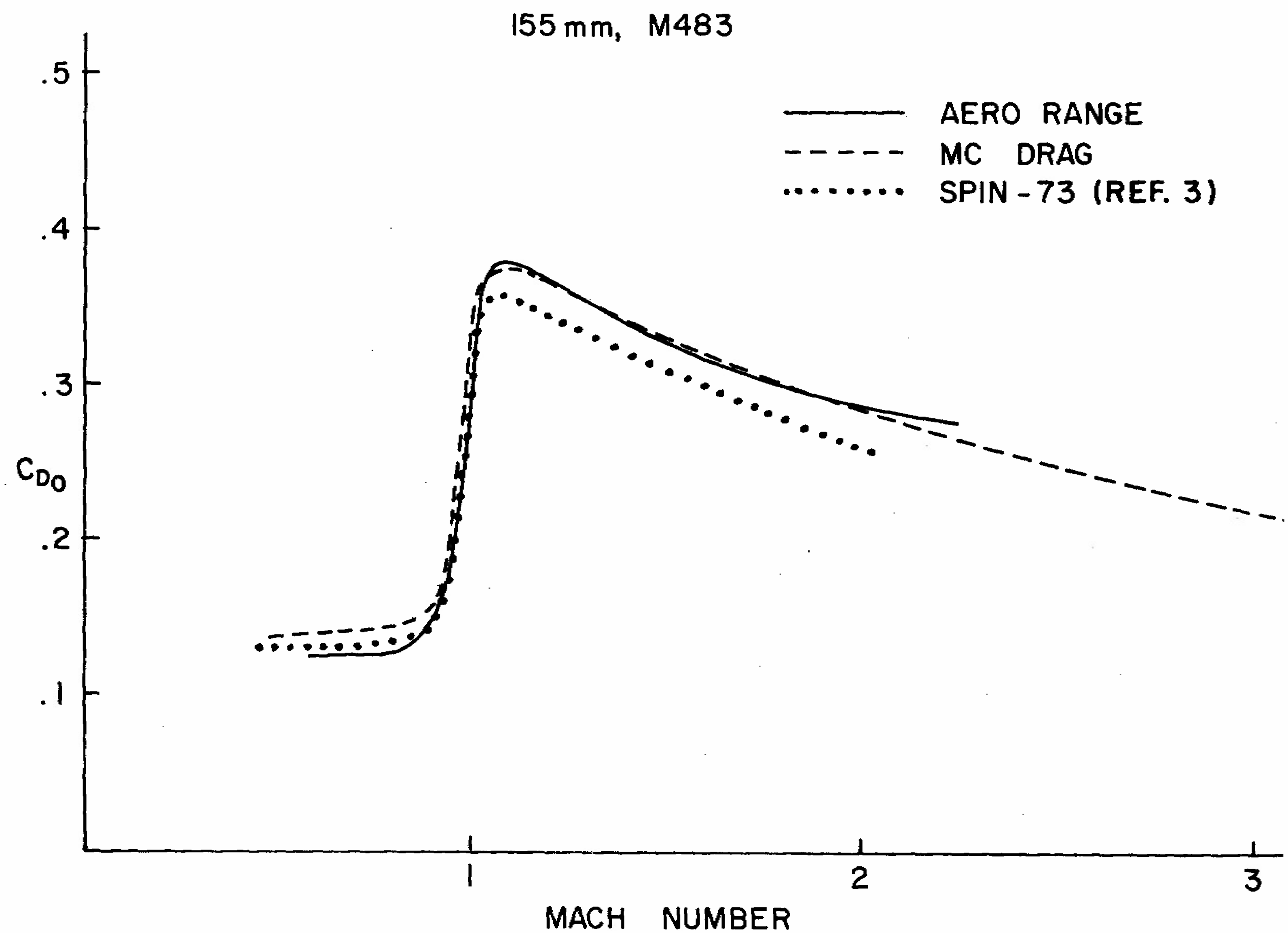

Figure 24. Drag Coefficient vs Mach Number, 155mm, M483

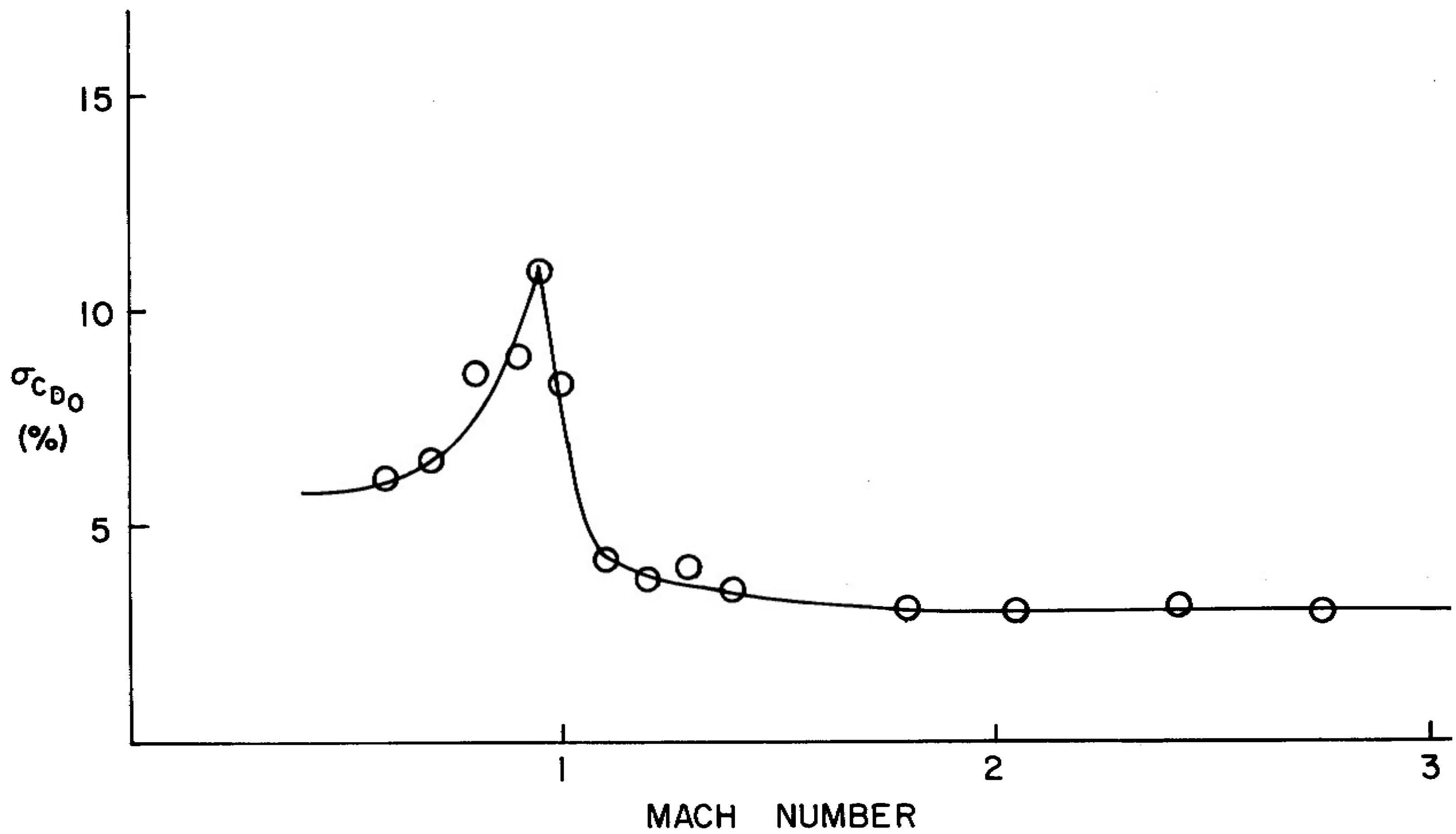

Figure 25. Standard Deviation of MC DRAG vs Mach Number

MC DRAG. DECEMBER 1974. R L MCCOY, LFD.

REF. DIA. (MM)	TOTAL LENGTH (CAL)	NOSE LENGTH (CAL)	RT/R	BOATTAIL LENGTH (CAL)	BASE DIA. (CAL)	MEPLAT DIA. (CAL)	BAND DIA. (CAL)	XCG. NOSE (CAL)	BOUND. LAYER CODE	IDENT
5.7	5.480	3.000	.50	1.000	.754	0.000	1.000	3.34	L/T	BRL-1

M	CD0	CDH	CDSF	CDBND	CDBT	CDB	PB/P1
.500	.112	0.000	.069	0.000	0.000	.043	.987
.600	.111	0.000	.065	0.000	0.000	.046	.980
.700	.111	0.000	.062	0.000	0.000	.049	.970
.800	.112	0.000	.059	0.000	0.000	.053	.958
.850	.113	0.000	.058	0.000	0.000	.055	.951
.900	.118	0.000	.057	0.000	.004	.056	.944
.925	.135	.013	.057	0.000	.008	.057	.940
.950	.158	.027	.056	0.000	.016	.058	.935
.975	.198	.039	.056	0.000	.044	.059	.931
1.000	.281	.051	.055	0.000	.090	.084	.896
1.100	.313	.119	.053	0.000	.056	.084	.875
1.200	.316	.106	.052	0.000	.075	.083	.853
1.300	.308	.099	.050	0.000	.077	.082	.829
1.400	.297	.093	.049	0.000	.074	.081	.804
1.500	.286	.090	.047	0.000	.070	.080	.779
1.600	.276	.086	.046	0.000	.066	.078	.754
1.700	.267	.084	.045	0.000	.062	.077	.728
1.800	.258	.081	.044	0.000	.058	.075	.702
2.000	.242	.078	.042	0.000	.052	.071	.652
2.200	.228	.075	.040	0.000	.047	.066	.604
2.500	.209	.071	.037	0.000	.041	.060	.538
3.000	.183	.066	.033	0.000	.034	.050	.449
3.500	.162	.063	.030	0.000	.028	.041	.383
4.000	.145	.060	.028	0.000	.023	.034	.334

Figure 26. MC DRAG Output for BRL-1

MC DRAG. DECEMBER 1974. R L MCCOY, LFD.

REF. DIA. (MM)	TOTAL LENGTH (CAL)	NOSE LENGTH (CAL)	RT/R	BOATTAIL LENGTH (CAL)	BASE DIA. (CAL)	MEPLAT DIA. (CAL)	BAND DIA. (CAL)	XCG, NOSE (CAL)	BOUND. LAYER CODE	IDENT
55.6	3.250	.967	0.00	1.180	1.630	.200	1.000	1.76	T/T	MIN/MAN

M	CD0	CDH	CDSF	CDBND	CDBT	CDB	PB/P1
.500	1.058	0.000	.043	0.000	0.000	1.014	.933
.600	1.059	0.000	.042	0.000	0.000	1.017	.904
.700	1.059	0.000	.040	0.000	0.000	1.019	.869
.800	1.057	0.000	.039	0.000	0.000	1.018	.828
.850	1.106	.050	.039	0.000	0.000	1.017	.806
.900	1.207	.132	.038	0.000	.021	1.016	.783
.925	1.262	.171	.038	0.000	.040	1.014	.771
.950	1.344	.207	.037	0.000	.087	1.013	.759
.975	1.523	.241	.037	0.000	.234	1.011	.747
1.000	1.885	.272	.037	0.000	.476	1.100	.710
1.100	1.948	.543	.036	0.000	.296	1.073	.658
1.200	2.565	.551	.035	0.000	.936	1.043	.604
1.300	2.291	.544	.034	0.000	.702	1.011	.550
1.400	2.131	.523	.033	0.000	.596	.978	.495
1.500	2.016	.505	.032	0.000	.535	.944	.441
1.600	1.925	.490	.032	0.000	.495	.909	.387
1.700	1.846	.477	.031	0.000	.466	.873	.335
1.800	1.776	.466	.030	0.000	.443	.837	.285
2.000	1.652	.448	.029	0.000	.410	.766	.193
2.200	1.544	.433	.028	0.000	.386	.698	.110
2.500	1.404	.415	.026	0.000	.360	.604	.006
3.000	1.217	.392	.023	0.000	.330	.472	-.120
3.500	1.075	.374	.021	0.000	.308	.372	-.201
4.000	.967	.360	.020	0.000	.291	.297	-.253

WARNING...NOSE TOO SHORT OR TOO BLUNT. CHECK CDH.

Figure 27. MC DRAG Output for 55mm Minuteman Model

MC DRAG, DECEMBER 1974, R L MCCOY, LFD.

REF. DIA. (MM)	TOTAL LENGTH (CAL)	NOSE LENGTH (CAL)	RT/R	BOATTAIL LENGTH (CAL)	BASE DIA. (CAL)	MEPLAT DIA. (CAL)	BAND DIA. (CAL)	XCG, NOSE (CAL)	BOUND. LAYER CODE	IDENT
155.0	5.650	3.010	.50	.580	.848	.090	1.020	3.53	T/T	M549

M	CD0	CDH	CDSF	CDBND	CDBT	CDB	PB/P1
.500	.129	0.000	.052	.000	0.000	.077	.981
.600	.131	0.000	.050	.000	0.000	.080	.972
.700	.133	0.000	.049	.000	0.000	.084	.960
.800	.137	0.000	.047	.001	0.000	.088	.945
.850	.139	0.000	.047	.003	0.000	.090	.937
.900	.147	0.000	.046	.005	.004	.092	.927
.925	.162	.009	.046	.008	.007	.093	.922
.950	.187	.022	.045	.010	.015	.094	.917
.975	.225	.034	.045	.010	.041	.095	.912
1.000	.309	.045	.045	.010	.084	.126	.877
1.100	.336	.107	.044	.009	.052	.125	.853
1.200	.327	.097	.042	.008	.056	.123	.827
1.300	.319	.092	.041	.008	.057	.121	.801
1.400	.309	.088	.040	.007	.054	.119	.773
1.500	.298	.085	.039	.007	.050	.117	.745
1.600	.288	.083	.039	.006	.047	.114	.716
1.700	.279	.080	.038	.006	.043	.111	.688
1.800	.270	.079	.037	.006	.041	.108	.659
2.000	.254	.075	.035	.006	.036	.102	.605
2.200	.239	.073	.034	.005	.032	.095	.553
2.500	.220	.070	.032	.005	.028	.085	.484
3.000	.192	.066	.029	.005	.023	.070	.390
3.500	.169	.063	.026	.005	.019	.057	.322
4.000	.152	.061	.024	.005	.016	.047	.272

Figure 28. MC DRAG Output for 155mm M549 Projectile

LIST OF REFERENCES

1. F. G. Moore, "Body Alone Aerodynamics of Guided and Unguided Projectiles at Subsonic, Transonic and Supersonic Mach Numbers," Naval Weapons Laboratory Technical Report TR-2796, November 1972. (AD 754098)

2. R. L. McCoy, "Estimation of the Static Aerodynamic Characteristics of Ordnance Projectiles at Supersonic Speeds," Ballistic Research Laboratories Report 1682, November 1973. (AD 771148)

3. R. H. Whyte, "SPIN-73, An Updated Version of the Spinner Computer Program," Picatinny Arsenal Contractor Report TR-4588, November 1973. (AD 915628L)

4. E. S. Sears, "An Empirical Method for Predicting Aerodynamic Coefficients for Projectiles - Drag Coefficient," Air Force Armament Laboratory Technical Report TR-72-173, August 1972. (AD 904587L)

5. G. I. Taylor and J. W. Maccoll, "The Air Pressure on a Cone Moving at High Speeds," Proc. Roy. Soc. A., Vol. 139 (1933), pp. 278-311.

6. M. J. Van Dyke, "The Similarity Rules for Second-Order Subsonic and Supersonic Flow," NACA Technical Note 3875, October 1956.

7. R. F. Clippinger, J. H. Giese and W. C. Carter, "Tables of Supersonic Flows ABout Cone Cylinders; Part I, Surface Data," Ballistic Research Laboratories Report 729, July 1950.

8. A. C. Charters and H. Stein, "The Drag of Projectiles with Truncated Cone Headshapes," Ballistic Research Laboratories Report 624, March 1952. (AD 800468)

9. E. R. Dickinson, "Some Aerodynamic Effects of Blunting a Projectile Nose," Ballistic Research Laboratories Memorandum Report 1596, September 1964. (AD 451977)

10. J. M. Wu, K. Aoyama and T. H. Moulden, "Transonic Flow Fields Around Various Bodies of Revolution Including Preliminary Studies on Viscous Effects With and Without Plume," U. S. Army Missile Command Report RD-TR-71-12, May 1971. (AD 729335)

11. J. D. Cole, G. E. Solomon and W. W. Willmarth, "Transonic Flows Past Simple Bodies," Journal of the Aeronautical Sciences, Vol. 20, No. 9, 1953, pp. 627-634.

12. H. W. Liepmann and A. Roshko, Elements of Gasdynamics, John Wiley and Sons, 1957.

13. R. Sedney, "Review of Base Drag," Ballistic Research Laboratories Report 1337, October 1966. (AD 808767)

14. J. Huerta, "An Experimental Investigation at Supersonic Mach Numbers of Base Drag of Various Boattail Shapes With Simulated Base Rocket Exhaust," Ballistic Research Laboratories Memorandum Report 1983, June 1969. (AD 855156)

15. D. M. Sykes, "Experimental Investigation of the Pressures on Boat-Tailed Afterbodies in Transonic Flow with a Low-Thrust Jet," Royal Armament Research and Development Establishment Memorandum 39/70, Fort Halstead, Kent, England, December 1970.

16. H. Schlichting, Boundary Layer Theory, McGraw-Hill, 1955.

17. E. R. Van Driest, "Turbulent Boundary Layers in Compressible Fluids," Journal of the Aeronautical Sciences, Vol. 18, No. 3, 1951, pp. 145-160, 216.

18. D. R. Chapman, "An Analysis of Base Pressure at Supersonic Velocities and Comparison with Experiment," NACA Report 1051, 1951.

19. G. P. Neitzel, Jr., "Aerodynamic Characteristics of 30mm HS831-L Ammunition Used in the British 30mm Rarden Gun," Ballistic Research Laboratories Memorandum Report 2466, March 1975. (AD B003797L)

20. E. R. Dickinson, "Some Aerodynamic Effects of Headshape Variation at Mach Number 2.44," Ballistic Research Laboratories Memorandum Report 838, October 1954. (AD 57748)

21. E. R. Dickinson, "Some Aerodynamic Effects of Varying the Body Length and Head Length of a Spinning Projectile," Ballistic Research Laboratories Memorandum Report 1664, July 1965. (AD 469897)

22. E. R. Dickinson, "The Effect of Boattailing on the Drag Coefficient of Cone-Cylinder Projectiles at Supersonic Velocities," Ballistic Research Laboratories Memorandum Report 842, November 1954. (AD 57769)

23. B. G. Karpov, "The Effect of Various Boattail Shapes on Base Pressure and Other Aerodynamic Characteristics of a 7-Caliber Long Body of Revolution at M = 1.70," Ballistic Research Laboratories Report 1295, August 1965. (AD 474352)

LIST OF REFERENCES (continued)

24. W. F. Braun, "Aerodynamic Data for Small Arms Projectiles," Ballistic Research Laboratories Report 1630, January 1973. (AD 909757L)

25. E. D. Boyer, "Free Flight Range Tests of a Minuteman Re-Entry Stage Model," Ballistic Research Laboratories Memorandum Report 1346, May 1961. (AD 326744)

26. R. Kline, W. R. Herrmann and V. Oskay, "A Determination of the Aerodynamic Coefficients of the 155mm, M549 Projectile," Picatinny Arsenal Technical Report 4764, November 1974. (AD B002073L)

APPENDIX

```
C     MC DRAG
C     ESTIMATE OF ZERO-YAW DRAG COEFFICIENT FOR A BODY OF REVOLUTION.
C     INPUTS ARE IN 5-DIGIT FIELDS, ON A SINGLE CARD, WITH COLS. 71-80
C     RESERVED FOR IDENTIFICATION.  READ IN. REFERENCE DIAMETER(MM).
C     TOTAL LENGTH(CAL). NOSE LENGTH(CAL). RATIO OF TANGENT RADIUS TO
C     ACTUAL NOSE RADIUS(HEADSHAPE PARAMETER), BOATTAIL LENGTH(CAL).
C     BASE DIAMETER(CAL). MEPLAT DIAMETER(CAL). BAND DIAMETER(CAL).
C     CENTER OF GRAVITY(CAL. FROM NOSE). BOUNDARY LAYER CODE(L/T OR T/T.
C     MUST BE IN COLS. 48-50), AND PROJECTILE IDENTIFICATION.
C     THE STANDARD DEVIATION OF THE DRAG ESTIMATE IS 10 PERCENT AT
C     SUBSONIC AND TRANSONIC SPEEDS, AND 4 PERCENT AT SUPERSONIC SPEEDS.
      DIMENSION CD(24),CDH(24),CDSF(24),CDBND(24),CDBT(24),CDB(24)
      DIMENSION PBP1(24)
      REAL M(24),LT,LN,LBT,M2
      DATA(M(I),I=1,24)/.5,.6,.7,.8,.85,.9,.925,.95,.975,1.,1.1,1.2,1.3,
     11.4,1.5,1.6,1.7,1.8,2.,2.2,2.5,3.,3.5,4./
    1 READ(5,501)DREF,LT,LN,RTR,LBT,DB,DM,DBND,XCGN,BLC,CODEA,CODEB
      WRITE(6,1501)
      WRITE(6,1502)
C     ECHO INPUT DATA
      WRITE(6,1503)
      WRITE(6,1504)
      WRITE(6,1505)
      WRITE(6,1506)DREF,LT,LN,RTR,LBT,DB,DM,DBND,XCGN,BLC,CODEA,CODEB
      IF(BLC.NE.3HL/T.AND.BLC.NE.3HT/T) GO TO 799
    2 DO 300 I=1,24
      TA=(1.-DM)/LN
      M2=M(I)**2
      RE=23296.3*M(I)*LT*DREF
      RET=.4343*(ALOG(RE))
      CFT=(.455/(RET**2.58))*((1.+.21*M2)**(-.32))
      DUM=1.+((.333+(.02/(LN**2)))*RTR)
      SWN=1.5708*LN*DUM*(1.+1./(8.*(LN**2)))
      SWCYL=3.1416*(LT-LN)
      SW=SWN+SWCYL
      IF(BLC.EQ.3HL/T)CFL=(1.328/(SQRT(RE)))*((1.+.12*M2)**(-.12))
      IF(BLC.EQ.3HT/T)CFL=CFT
      CDSFL=1.2732*SW*CFL
      CDSFT=1.2732*SW*CFT
      CDSF(I)=(CDSFL*SWN+CDSFT*SWCYL)/SW
      CHI=(M2-1.)/(2.4*M2)
      IF(M(I).LE.1.)PTP=(1.+.2*M2)**3.5
      IF(M(I).GT.1.)PTP=((1.2*M2)**3.5)*((6./(7.*M2-1.))**2.5)
      CMEP=(1.122*(PTP-1.)*(DM*DM))/M2
      IF(M(I).LE..91)CDHM=0.
      IF(M(I).GE.1.41)CDHM=.85*CMEP
      IF(M(I).GT..91.AND.M(I).LT.1.41)CDHM=(.254+2.88*CHI)*CMEP
      IF(M(I).LT.1.)PB2=1./(1.+.1875*M2+.0531*M2*M2)
      IF(M(I).GE.1.)PB2=1./(1.+.2477*M2+.0345*M2*M2)
      PB4=(1.+.09*M2*(1.-EXP(LN-LT)))*(1.+.25*M2*(1.-DB))
      PBP1(I)=PB2*PB4
      CDB(I)=(1.4286*(1.-PBP1(I))*(DB*DB))/M2
      IF(M(I).LT..95)CDBND(I)=(M(I)**12.5)*(DBND-1.)
      IF(M(I).GE..95)CDBND(I)=(.21+.28/M2)*(DBND-1.)
      IF(M(I)-1.)100,100,200
```

```
C        100 NO. INSTRUCTIONS FOR SUBSONIC-TRANSONIC SPEEDS.
  100  IF(LBT)102,101,102
  101  CDBT(I)=0.
       GO TO 105
  102  IF(M(I).LE..85) GO TO 101
       TB=(1.-DB)/(2.*LBT)
       TB23=2.*TB*TB+(TB**3)
       EBT=EXP((-2.)*LBT)
       BBT=1.-EBT+2.*TB*((EBT*(LBT+.5))-.5)
       CDBT(I)=2.*TB23*BBT*(1./(.564+1250.*CHI*CHI))
  105  XMC=(1.+.552*(TA**.8))**(-.5)
       IF(M(I).LE.XMC)CDHT=0.
       IF(M(I).GT.XMC)CDHT=.368*(TA**1.8)+1.6*TA*CHI
       CDH(I)=CDHT+CDHM
       GO TO 300
C        200 NO. INSTRUCTIONS FOR SUPERSONIC SPEEDS.
  200  BE2=M2-1.
       BE=SQRT(BE2)
       ZE=BE
       SSMC=1.+.358*(TA**1.85)
       IF(M(I).LT.SSMC)ZE=SQRT(SSMC*SSMC-1.)
       C1=.7156-.5313*RTR+.595*(RTR**2)
       C2=.0796+.0779*RTR
       C3=1.587+.049*RTR
       C4=.1122+.1658*RTR
       RZ2=1./(ZE*ZE)
       CDHT=(C1-C2*(TA**2))*RZ2*((TA*ZE)**(C3+C4*TA))
       CDH(I)=CDHT+CDHM
       IF(LBT)202,201,202
  201  CDBT(I)=0.
       GO TO 300
  202  TB=(1.-DB)/(2.*LBT)
       IF(M(I)-1.1) 205,205,207
  205  TB23=2.*TB*TB+(TB**3)
       EBT=EXP((-2.)*LBT)
       BBT=1.-EBT+2.*TB*((EBT*(LBT+.5))-.5)
       CDBT(I)=2.*TB23*BBT*(1.774-9.3*CHI)
       GO TO 300
  207  BB=.85/BE
       AA2=(5.*TA)/(6.*BE)+(.5*TA)**2-(.7435/M2)*((TA*M(I))**1.6)
       AA1=(1.-((.6*RTR)/M(I)))*AA2
       EXL=EXP(((-1.1952)/M(I))*(LT-LN-LBT))
       XXM=((2.4*M2*M2-4.*BE2)*(TB*TB))/(2.*BE2*BE2)
       AA=AA1*EXL-XXM+((2.*TB)/BE)
       RB=1./BB
       EXBT=EXP((-BB)*LBT)
       AAB=1.-EXBT+(2.*TB*(EXBT*(LBT+RB)-RB))
       CDBT(I)=4.*AA*TB*AAB*RB
  300  CONTINUE
       WRITE(6,1502)
```

```
      DO 305 I=1,24
      CD(I)=CDH(I)+CDSF(I)+CDBND(I)+CDBT(I)+CDB(I)
  305 WRITE(6,1509)M(I),CD(I),CDH(I),CDSF(I),CDBND(I),CDBT(I),CDB(I),[illegible]
     11(I)
      WRITE(6,1511)
      IF(LN.LT.1..OR.DM.GT..5) GO TO 698
  310 IF(LBT.GT.1.5.OR.DB.LT..65) GO TO 699
      GO TO 1
  698 WRITE(6,1512)
      GO TO 310
  699 WRITE(6,1513)
      GO TO 1
  799 BLC=3HT/T
      WRITE(6,1507)
      GO TO 2
  501 FORMAT(9F5.3,2X,A3,20X,2A5)
 1501 FORMAT(1H1)
 1502 FORMAT(42H MC DRAG, DECENPER 1974, R L MCCOY, LFD.//)
 1503 FORMAT(77H REF.   TOTAL     NOSE    RT/R BOATTAIL BASE   MEPLAT   BAND
     1  XCG, BOUND.   IDENT)
 1504 FORMAT(68H DIA.   LENGTH  LENGTH          LENGTH  DIA.    DIA.    DIA.
     1  NOSE LAYER)
 1505 FORMAT(68H (MM)   (CAL)    (CAL)           (CAL)    (CAL) (CAL)    (CAL)
     1 (CAL)  CODE/)
 1506 FORMAT(F6.1,F7.3,F8.3,F6.2,F8.3,F7.3,F6.3,F8.3,F6.2,2X,A3,3X,2A5//
     1/)
 1507 FORMAT(56H ILLEGAL BOUNDARY LAYER CODE. ALL TURBULENT B/L ASSUMED.
     1//)
 1508 FORMAT(55H   M      CD0     CDH     CDSF   CDBND    CDBT    CDB    PB/PI/
     1)
 1509 FORMAT(F6.3,7F7.3)
 1511 FORMAT(///)
 1512 FORMAT(50H WARNING...NOSE TOO SHORT OR TOO BLUNT. CHECK CDH./)
 1513 FORMAT(54H WARNING...BOATTAIL TOO LONG OR TOO STEEP. CHECK CDBT.)
      END
```

LIST OF SYMBOLS

a_∞	Speed of sound in the free stream
A	Change in boattail pressure coefficient due to a Prandtl-Meyer expansion
A_1	Headshape correction factor for supersonic boattail drag coefficient
BLC	Boundary layer code in "MC DRAG" input
C_1, C_2, C_3, C_4	Correlation parameters for head drag coefficient
C_{D_0}	Total drag coefficient at zero angle of attack
C_{D_H}	Pressure drag coefficient due to projectile head (nose)
$C_{D_{BT}}$	Pressure drag coefficient due to boattail (or flare)
C_{D_B}	Pressure drag coefficient due to the blunt nose
$C_{D_{BND}}$	Pressure drag coefficient due to a rotating band
$C_{D_{SF}}$	Skin friction drag coefficient
C_F	Skin friction coefficient for a smooth flat plate
C_{f_L}	Laminar skin friction coefficient
C_{f_T}	Turbulent skin friction coefficient
C_{p_s}	Stagnation pressure coefficient
d_B	Projectile base diameter (calibers)
d_{RB}	Rotating band diameter (calibers)
d_M	Meplat diameter (calibers)
d_{REF}	Projectile reference diameter (mm)

f( )	Denotes a functional dependence on the quantity ( )
F( )	Denotes a functional dependence on the quantity ( )
k	Boattail pressure recovery factor
K	Stagnation pressure correction coefficient
ℓ	Projectile total length (mm)
L_{BT}	Boattail (or flare) length (calibers)
L_{CYL}	Projectile cylinder length (calibers)
L_N	Projectile nose length (calibers)
$\hat{L}_N$	Length of nose if extended to a sharp point (calibers)
M_c	Critical Mach number for the onset of transonic flow
M_∞	Free stream Mach number
P_∞	Free stream static pressure
P_B	Base pressure
R	Ogive radius of projectile nose (calibers)
R_T	Tangent ogive radius (calibers)
Re_ℓ	Reynolds number, based on projectile length
S_W	Projectile wetted surface area (calibers^2)
U_∞	Free stream speed
X_{CG}	Center of gravity location (calibers from nose)
β	Boattail angle
γ	Ratio of specific heats
ν	Kinematic viscosity
τ	Nose thickness ratio

DISTRIBUTION LIST

No. of Copies	Organization
12	Commander Defense Technical Info Center ATTN: DDC-DDA Cameron Station Alexandria, VA 22314
1	Commander US Army Materiel Development and Readiness Command ATTN: DRCDMD-ST 5001 Eisenhower Avenue Alexandria, VA 22333
2	Commander US Army Armament Research and Development Command ATTN: DRDAR-TSS Dover, NJ 07801
11	Commander US Army Armament Research and Development Command ATTN: DRDAR-LCA-F Mr. A. Loeb DRDAR-LCA-FA Mr. S. Wasserman Mr. D. Mertz DRDAR-LCA-FB Mr. R. Kline Mr. E. Falkowski Mr. S. Kahn Mr. H. Hudgins Mr. E. Friedman Mr. C. Ng DRDAR-LCA Mr. W. R. Benson DRDAR-LCV Mr. R. Reisman Dover, NJ 07801
8	Commander US Army Armament Research and Development Command ATTN: DRDAR-SCA-SC COL M. G. Swindler DRDAR-SC Mr. E. Malatesta DRDAR-SCA-AC Mr. R. Schlenner Mr. R. Rhodes Mr. R. Heredia DRDAR-SCA-A Mr. R. Reagan DRDAR-SCS-E Mr. A. Mancini DRDAR-SC Mr. J. Steiner Dover, NJ 07801
1	Commander US Army Armament Readiness Command ATTN: DRSAR-LEP-L, Tech Lib Rock Island, IL 61299
1	Director US Army Armament Research and Development Command Benet Weapons Laboratory ATTN: DRDAR-LCB-TL Watervliet, NY 12289
1	Commander US Army Aviation Research and Development Command ATTN: DRSAV-E P.O. Box 209 St. Louis, MO 63166
1	Director US Army Air Mobility Research and Development Laboratory Ames Research Center Moffett Field, CA 94035

DISTRIBUTION LIST

No. of Copies	Organization
1	Commander US Army Electronic Research and Development Command Technical Support Activity ATTN: DELSD-L Fort Monmouth, NJ 07703
1	Commander US Army Missile Command ATTN: DRSMI-R Redstone Arsenal, AL 35898
1	Commander US Army Missile Command ATTN: DRSMI-YDL Redstone Arsenal, AL 35898
2	Commander US Army Missile Command ATTN: DRSMI-RDK Mr. R. A. Deep Mr. W. D. Washington Redstone Arsenal, AL 35898
1	Commander US Army Communications Research and Development Command ATTN: DRDCO-PPA-SA Fort Monmouth, NJ 07703
1	Commander US Army Tank Automotive Research and Development Command ATTN: DRDTA-UL Warren, MI 48090
1	Commander US Army Yuma Proving Ground ATTN: STEYP-TMW Mr. W. T. Vomocil Yuma, AZ 85364

No. of Copies	Organization
1	Commander US Army Research Office ATTN: CRD-AA-EH P.O. Box 12211 Research Triangle Park NC 27709
1	Commander US Army Standardization Group, UK Box 65 FPO New York 09510
2	Chief US Army Standardization Group ATTN: DAMA-PPI, COL Noce National Defense Headquarters Ottawa, Ontario, Canada KIA OK2
3	Chief US Army Standardization Group, Australia San Francisco, CA APO 96404
1	Director US Army TRADOC Systems Analysis Activity ATTN: ATAA-SL, Tech Lib White Sands Missile Range NM 88002
1	Commander Naval Air Systems Command ATTN: AIR-604 Washington, DC 20360
1	Commander David W. Taylor Naval Ship Research and Development Center ATTN: Aerodynamics Laboratory Bethesda, MD 20084

DISTRIBUTION LIST

No. of Copies	Organization
1	Commander Naval Air Development Center, Johnsville Warminster, PA 18974
3	Commander Naval Ordnance Systems Command ATTN: ORD-0632 ORD-035 ORD-5524 Washington, DC 20360
1	Superintendent Naval Postgraduate School Monterey, CA 93940
5	Commander Naval Surface Weapons Center ATTN: Dr. Thomas Clare Dr. W. R. Chadwick Dr. W. G. Soper Dr. F. Moore Dr. T. R. Pepitone Dahlgren, VA 22448
1	Commander Naval Surface Weapons Center ATTN: Code 730, Tech Lib Silver Spring, MD 20910
1	Commander Naval Research Laboratory ATTN: Tech Info Div Washington, DC 20375
1	Commander Naval Weapons Center ATTN: Code 233 China Lake, CA 93555
1	AFATL (Tech Lib) Eglin AFB, FL 32542
4	AFATL/DLDL ATTN: Dr. D. C. Daniel Mr. K. Cobb Mr. G. Winchenbach Mr. K. West Eglin AFB, FL 32542
2	Air Proving Ground Center (PGTRI) ATTN: Mr. C. Butler Mr. E. Sears Eglin AFB, FL 32542
1	AFFDL Wright-Patterson Air Force Base OH 45433
1	ASD (ASAMCG) Wright-Patterson Air Force Base OH 45433
4	Director Sandia Laboratories ATTN: Division 1342, Mr. W. F. Hartman Division 1331, Mr. H. R. Vaughn Mr. A. E. Hodapp Mr. W. Curry Albuquerque, NM 87115
4	Director National Aeronautics and Space Administration Ames Research Center ATTN: Dr. Gary Chapman Mr. A. Seiff Mr. Murray Tobak Tech Lib Moffett Field, CA 94035

DISTRIBUTION LIST

No. of Copies	Organization
1	Director National Aeronautics and Space Administration George C. Marshall Space Flight Center ATTN: MS-I, Library Huntsville, AL 35812
1	Director National Aeronautics and Space Administration Langley Research Center ATTN: MS 185, Tech Lib Langley Station Hampton, VA 23365
1	Director National Aeronautics and Space Administration Lewis Research Center ATTN: Tech Lib 21000 Brookpark Road Cleveland, OH 44135
1	Director National Aeronautics and Space Administration Scientific and Technical Information Facility P.O. Box 8757 Baltimore/Washington International Airport, MD 21240
1	Director Applied Physics Laboratory The Johns Hopkins University Johns Hopkins Road Laurel, MD 20810
1	Alpha Research, Inc. ATTN: Mr. J. E. Brunk P.O. Box U Santa Barbara, CA 93102
1	Aerospace Corporation ATTN: Dr. Daniel Platus 2350E El Segundo Avenue El Segundo, CA 90245
1	Calspan Corporation P.O. Box 400 Buffalo, NY 14221
1	Chrysler Corporation - Defense Division ATTN: Dr. R. Lusardi Detroit, MI 48231
1	Technical Director Colt Firearms Corporation 150 Huyshope Avenue Hartford, CT 14061
1	General Dynamics Corporation ATTN: Electro-Dynamics Div. Dr. D. L. Trulin P.O. Box 2507 Pomona, CA 91766
1	General Electric Company Armament Systems Department ATTN: Mr. Robert H. Whyte Lakeside Avenue Burlington, VT 05401
1	Honeywell, Incorporated Government & Aerospace Products Division ATTN: Mail Station MN 112190 G. Stilley 600 Second Street, North Hopkins, MN 55343
2	Hughes Helicopter ATTN: Mr. R. Land Mr. B. Lindner Centinella and Teale Streets Culver City, CA 90230

DISTRIBUTION LIST

No. of Copies	Organization
2	Martin Marietta Aerospace Orlando Division ATTN: MP-334 Mr. P. Morrison Mr. W. Appich Orlando, FL 32805
1	National Rifle Association of America ATTN: Mr. C. E. Harris 1600 Rhode Island Avenue Washington, DC 20036
3	Nielsen Engineering and Research, Incorporated ATTN: Dr. J. N. Nielsen Dr. J. R. Spreiter Dr. S. S. Stahara Mountain View, CA 94043
1	Olin Corporation Winchester-Western Division 275 Winchester Avenue New Haven, CT 06504
1	Olin Corporation ATTN: Mr. D. Marlow P.O. Drawer G Marion, IL 62959
1	Remington Arms Company, Incorporated Bridgeport, CT 06602
1	University of Delaware ATTN: Dept. of Mechanical and Aerospace Engineering Dr. J. Danberg Newark, DE 19711
1	University of Maryland ATTN: Mathematics Department Prof. Y. M. Lynn 5401 Wilkins Avenue Baltimore, MD 21228

No. of Copies	Organization
1	University of Notre Dame ATTN: Dept.Aerospace Eng. Dr. T. J. Mueller South Bend, IN 46556
1	University of Tennessee Space Institute ATTN: Dr. J. M. Wu Tullahoma, TN 37388
1	University of Texas-Austin ATTN: Dept. Mech. Eng. Dr. W. Oberkampf Austin, TX 78712
1	University of Virginia Department of Engineering Science and Systems ATTN: Prof. Ira D. Jacobson Thornton Hall Charlottesville, VA 22904

Aberdeen Proving Ground

Dir, USAMSAA
ATTN: DRXSY-D
DRXSY-MP, H. Cohen

Cdr, USATECOM
ATTN: DRSTE-TO-F

Dir, USACSL, Bldg. E3516
ATTN: DRDAR-CLB-PA